

Beyond maps: Patterns of formation processes at the Middle Pleistocene open-air site of Marathousa 1, Megalopolis Basin, Greece

D. Giusti^{a,*}, V. Tourloukis^a, G. E. Konidaris^a, N. Thompson^a, P. Karkanas^c,
E. Panagopoulou^d, K. Harvati^a

^a*Paläoanthropologie, Senckenberg Centre for Human Evolution and Palaeoenvironment, Eberhard Karls Universität Tübingen, Rümelinstr. 23, 72070 Tübingen, Germany*

^b*Friedrich-Alexander University of Erlangen-Nürnberg, Institute of Prehistory and Early History, Kochstr. 4/18, 90154 Erlangen, Germany*

^c*Malcolm H. Wiener Laboratory for Archaeological Science, American School of Classical Studies at Athens, Greece*

^d*Ephoreia of Palaeoanthropology-Speleology of Greece, Athens, Greece*

Abstract

Recent excavations at the Middle Pleistocene open-air site of Marathousa 1 have unearthed in one of the two investigated areas (Area A) a partial skeleton of a single individual of *Elephas (Palaeoloxodon) antiquus* and other faunal remains in spatial and stratigraphic association with lithic artefacts. In Area B, a much higher number of lithic artefacts was collected, spatially and stratigraphically associated with other faunal remains. The two areas are stratigraphically correlated, the main fossiliferous layers representing an *en masse* depositional process in a lake margin context. Evidence of butchering (cut-marks) has been identified on two bones of the elephant skeleton, as well on other mammal bones from Area B. However, due to the secondary deposition of the main find-bearing units, it is of primary importance to evaluate the degree and reliability of the spatial association of the lithic artefacts with the faunal remains. Indeed, spatial association does not necessarily imply causation: natural syn- and post-depositional processes may equally produce spatial association. Assessing the extent of post-depositional reworking processes is crucial to fully comprehend the archaeological record, and therefore to reliably interpret past human behaviours. The present

*Corresponding author

Email address: domenico.giusti@uni-tuebingen.de (D. Giusti)

study uses a comprehensive set of spatial statistics in order to disentangle the depositional processes behind the distribution of the archaeological and palaeontological record at Marathousa 1. Results of our analyses suggest minor reworking and substantial spatial association of the lithic and faunal assemblages, supporting the current interpretation of Marathousa 1 as a butchering site.

Keywords: Spatial taphonomy, Site formation processes, Vertical distribution, Fabric analysis, Point pattern analysis, Middle Pleistocene

1. Introduction

Archaeological site formation processes, intensively studied since the early 1970s (Isaac, 1967; Schiffer, 1972, 1983, 1987; Shackley, 1978; Wood and Johnson, 1978; Schick, 1984, 1986, 1987; Petraglia and Nash, 1987; Petraglia and Potts, 1994, among others), “still insufficiently taken in consideration” (?) at the beginning of the 21st century, are nowadays fully acknowledged in the archaeological practice (???Malinsky-Buller et al., 2011; Vaquero et al., 2012; Bargalló et al., 2016, among others). Drawing inferences about past human behaviours from scatters of archaeological remains must account for syn- and post-depositional contextual processes.

Several methods are currently applied in order to qualify and quantify the type and degree of reworking of archaeological assemblages. Within the framework of a geoarchaeological and taphonomic approach, spatial statistics offer meaningful contributions in unravelling site formation and modification processes from spatial patterns. However, while the spatio-temporal dimension is an ineluctable inherent property of any biotic or abiotic process, spatial statistics are still insufficiently taken in consideration.

Distribution maps are cornerstones of the archaeological documentation process and are primary analytic tools. However, their visual interpretation is prone to subjectivity and is not reproducible (Bevan et al., 2013). Since the early 1970’s (see Hodder and Orton (1976); Orton (1982) and references therein), the traditional, intuitive, ‘eyeballing’ method of spotting spatial patterns has been abandoned in favour of more objective approaches, extensively borrowed from other fields. Nevertheless, quantitative methods, while still percolating in the archaeological sciences from neighbouring dis-

23 ciplines, are not extensively used. Moreover, only a relatively small number of studies
24 have explicitly applied spatial point pattern analysis or geostatistics to the study of site
25 formation and modification processes (Lenoble et al. (2008); Domínguez-Rodrigo et al.
26 (2014b,a, 2017); Carrer (2015); Giusti and Arzarello (2016); Organista et al. (2017) -
27 but see Hivernel and Hodder (1984) for an earlier work on the subject).

28 The goal of a taphonomic approach to spatial analysis is to move beyond distri-
29 bution maps by applying a comprehensive set of multiscale and multivariate spatial
30 statistics in order to reliably construct inferences from spatial patterns. An exhaustive
31 spatial analytic approach to archaeological inference, combined with a taphonomic
32 perspective, is essential for evaluating the depositional processes and integrity of the
33 archaeological assemblage, and consequently for a reliable interpretation of past hu-
34 man behaviours.

35 The present study uses a comprehensive set of spatial analyses (fabric, vertical dis-
36 tribution and point pattern analyses) in order to disentangle the depositional processes
37 behind the spatial distribution of the archaeological and palaeontological record re-
38 covered during excavation at the Middle Pleistocene open-air site of Marathousa 1,
39 Megalopolis, Greece (Panagopoulou et al., 2015; Harvati et al., 2016).

40 *1.1. Marathousa 1*

41 The site (Fig. 1), discovered in 2013 at the edge of an active lignite quarry (Thomp-
42 son et al., this issue), is located between two lignite seams in the Pleistocene deposits
43 of the Megalopolis basin, Marathousa Member of the Choremi Formation (van Vugt
44 et al., 2000). The regular alternation of lacustrine clay, silt and sand beds with lignite
45 seams has been interpreted having cyclic glacial (or stadial) and interglacial (or inter-
46 stadial) origin (Nickel et al., 1996). The half-graben configuration of the basin, with
47 major subsidence along the NW-SE trending normal faults along the eastern margin,
48 resulted in the gentle dip of the lake bottom at the opposite, western, margin of the
49 lake, enabling the formation of swamps and the accumulation of organic material for
50 prolonged periods of time (van Vugt et al., 2000).

51 Two excavation areas have been investigated since 2013: Area A, where several
52 skeletal elements of a single individual of *Elephas (Palaeoloxodon) antiquus* have been

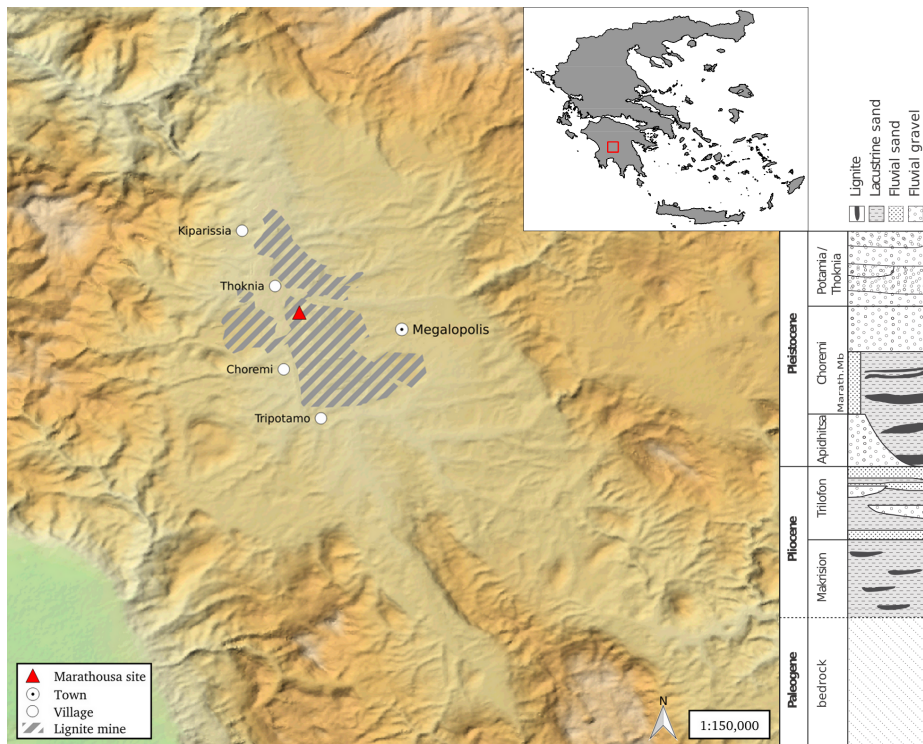


Figure 1: Geographical location of the Marathousa 1 site in the Megalopolis basin and stratigraphic column, modified after [van Vugt et al. \(2000\)](#).

53 unearthened, together with a number of lithic artefacts (Konidaris et al., this issue; Tour-
54 loukis et al., this issue); and Area B, located 60 m to the South along the exposed
55 section, where the lithic assemblage is richer and occurs in association with a faunal
56 assemblage composed of isolated elephant bones, cervids and carnivores among others
57 (Fig. ??). Evidence of butchering (cut-marks) have been identified on two of the ele-
58 phant bones from Area A, as well on elephant and other mammal bones from Area B
59 (Konidaris et al., this issue).

60 The sedimentary sequence of the site (Fig. 3) includes lacustrine and fluvio-lacustrine
61 clastic deposits between lignite seams II (UA7-UB10) and III (UA1-UB1) (Karkanas
62 et al., Tourloukis et al., this issue). A major hiatus (UA3/4, UB5/6), attributed to ex-
63 posure and erosion of a lake shore mudflat, divides the sequence in two parts. The
64 lower part is characterized by high rate subaqueous sedimentation of bedded sands and
65 silts; while the upper one is characterized by a series of erosional bounded depositional
66 units, attributed to subaerial organic- and carbonate-rich mudflows and hyperconcen-
67 trated flows (Karkanas et al., this issue).

68 The erosional contacts UA3c/4 and UB4c/5a separate the two main find-bearing
69 units in both areas. In Area A, the elephant remains lie at the contact of UA3c/4 and
70 are covered by UA3c (Fig. 4); while in Area B, most of the remains were collected
71 from unit UB4c. Units UA3c and UB4c (organic-rich, intraclast-rich silty sands) re-
72 semble dilute mudflows, showing a chaotic structure of rip-up clasts from the underly-
73 ing sediment and small-to-large wood fragments. In Area B, channelized sands (UB5),
74 probably not preserved in Area A, begin the upper part of the sequence. A relatively
75 low number of remains was found in massive organic-rich silty sands (UB5a), which
76 locally overlay these channelized sands (Karkanas et al., this issue).

77 For both areas, the working hypothesis is that the flow event represented by units
78 UA3c and UB4c eroded and scoured the exposed surface (where the elephant was ly-
79 ing), thereby entraining clastic material (including probably artefacts) and re-depositing
80 this material at a close distance (see Karkanas et al., this issue).

81 The erosional event described above, and specifically the erosional contacts be-
82 tween the fossiliferous horizons in the two areas, provide the essential background for
83 the analysis and interpretation of the spatial distributions at Marathousa 1.

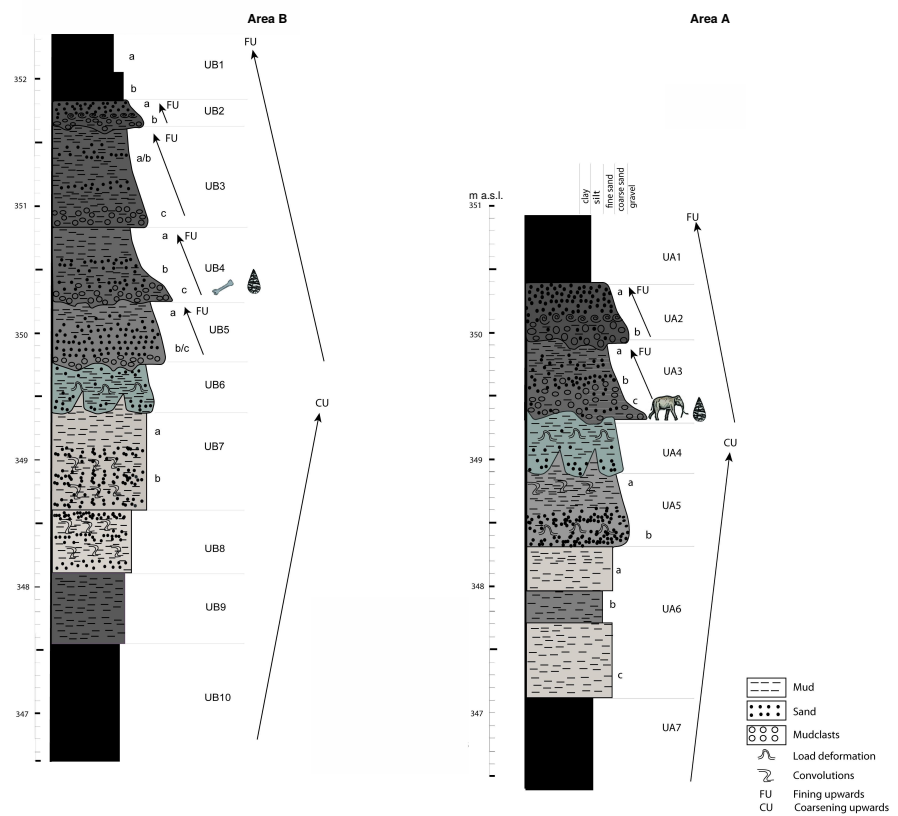


Figure 2: Stratigraphic setting of the Marathousa 1 site, modified after Karkanas et al. (this issue).

84 The secondary depositional nature of the main find horizons raises the question
85 of how reliable is the spatial association between the lithic artefacts and the partial
86 skeleton of a single *Elephas (Palaeoloxodon) antiquus* individual and other faunal
87 remains. Since spatial association does not necessarily imply causation, and conse-
88 quently synchrony (?), the answer has important consequences for the interpretation
89 of the site in the broader context of the Middle Pleistocene human-proboscidean inter-
90 actions. We aim to tackle this question and disentangle the formation processes acting
91 at Marathousa 1 on the basis of spatial patterns through a three-prong spatial analytic
92 approach:

- 93 1. by analysing, in a frame of references, the fabric of remains from relevant strati-
94 graphic units;
- 95 2. by quantifying and comparing their relative vertical distributions;
- 96 3. by identifying spatial trends in either the assemblage intensities and the associa-
97 tions between classes of remains.

98 **2. Material and methods**

99 Since 2013, systematic investigation of the Marathousa 1 site has been carried out
100 by a joint team from the Ephoreia of Palaeoanthropology-Speleology (Greek Ministry
101 of Culture) and the University of Tübingen. A grid system of 1 square meter units
102 was set up, oriented -14 degrees off the magnetic North, and including the two areas
103 of investigation. The excavation of the deposit proceeded in 50x50 cm sub-squares
104 in Area B and 1x1 m squares in Area A, and spits of 5 to 10 cm thickness, respec-
105 tively. Systematic water-screening of sediments was carried out on-site using 1 mm
106 sieves in order to guarantee recovery of the small-size fraction (e.g., micro-artefacts,
107 small mammal remains, fish, molluscs and small fragments of organic and inorganic
108 material). The three-dimensional coordinates of finds (i.e., all the lithic artefacts, teeth
109 and diagnostic bones; bones and organic material with a-axis \geq 20 mm), collected
110 spits of sediment, samples and geological features (e.g., erosional contacts and mud
111 cracks) were recorded with a Total Station. Dense clouds of surface points of the Ele-
112 phant skeletal elements were acquired using both a Total Station and a close-range

photogrammetric technique. The dimensions (length, width and thickness) of registered finds were measured on-site with millimetre rules. Orientation (dip and strike) of elongated particles (i.e., faunal remains, large wood fragments and lithic artefacts) was recorded since 2013 with a 30 degree accuracy, using a clock-like system (the strike was measured, relatively to the grid North, in twelve clockwise intervals). In 2015, the use of a compass and inclinometer with an accuracy of 1 degree was introduced in Area B to gradually replace the former method. Strike (azimuth) and dip measurements were taken along the symmetrical longitudinal a-axis (SLA) of the bones ([Domínguez-Rodrigo and García-Pérez, 2013](#)), the lithic artefacts ([Bertran and Texier, 1995](#)) and organic material, using the lowest endpoint of the axis as an indicator of the vector direction.

The present study focuses on the excavated stratigraphic units in which most of the archaeological and palaeontological remains were recovered in both excavation areas, namely in UA3c and UA4 in Area A, and UB4c and UB5a in Area B. From the total, subset samples of material were used for each specific spatial analysis. For the fabric analysis we included material collected until 2016. For the vertical distribution and point pattern analyses, the region of investigation was limited to the squares excavated from 2013 until 2015, 25 and 29 square meters respectively in each area.

The analyses were performed in R statistical software ([R Core Team, 2016](#)). In order to make this research reproducible ([Marwick, 2017](#)), a repository containing a compendium of data, source code and text is open licensed and available at the DOI: [10.5281/zenodo.822273](https://doi.org/10.5281/zenodo.822273)

2.1. Fabric analysis

The study of clast fabric (i.e., the orientation pattern of elongated sedimentary particles, including bones and artefacts), first addressed by [Voorhies \(1966\)](#); [Isaac \(1967\)](#); [Bar-Yosef and Tchernov \(1972\)](#); [Schick \(1986\)](#), has more recently been found to successfully discriminate between different sedimentary processes ([Bertran and Texier, 1995](#); [Bertran et al., 1997](#)), leading to a noteworthy development of methods and propagation of applications in Palaeolithic site formation studies ([Lenoble and Bertran, 2004](#); [Lenoble et al., 2008](#); [McPherron, 2005](#); [Benito-Calvo et al., 2009, 2011](#); [Benito-](#)

¹⁴³ Calvo and de la Torre, 2011; Bernatchez, 2010; Boschian and Saccà, 2010; Domínguez-
¹⁴⁴ Rodrigo et al., 2012; Domínguez-Rodrigo and García-Pérez, 2013; Domínguez-Rodrigo
¹⁴⁵ et al., 2014c; de la Torre and Benito-Calvo, 2013; Walter and Trauth, 2013; García-
¹⁴⁶ Moreno et al., 2016; Sánchez-Romero et al., 2016, among others).

¹⁴⁷ Comparative fabric analysis was conducted with the aim to investigate the dynamics
¹⁴⁸ of the depositional processes at Marathousa 1. The analysis of the orientation of
¹⁴⁹ elongated clasts can distinguish three main types of pattern (isotropic, planar and linear
¹⁵⁰ fabric), each associated with different sedimentary processes.

¹⁵¹ At the margin of a lacustrine environment, relatively close to the surrounding relief,
¹⁵² a combination of high- and low-energy processes can be expected. According to
¹⁵³ the depositional context of the site (Karkanas et al., this issue), a strong preferred ori-
¹⁵⁴ entation of clasts (linear pattern) would suggest the action of massive slope processes
¹⁵⁵ such as mudslides and debris / hyperconcentrated flows. On the other hand, whereas
¹⁵⁶ the frontal lobes of debris flows have been found to show a more random orientation
¹⁵⁷ (isotropic pattern), overland flows have been associated with planar fabrics (Lenoble
¹⁵⁸ and Bertran, 2004). Conversely, in a lacustrine floodplain, anisotropy without signif-
¹⁵⁹ icant transport can be caused by low-energy processes such as lake transgression and
¹⁶⁰ regression, as well as water-sheet flows formed during rainy seasons. Isotropic patterns
¹⁶¹ have been observed in different parts of mudflats as well (Cobo-Sánchez et al., 2014).

¹⁶² Nevertheless, grey zones exist between different depositional processes, so that an
¹⁶³ unequivocal discrimination based only on fabric observations is often not possible, and
¹⁶⁴ other taphonomic criteria must also be considered ()�.

¹⁶⁵ Since fabric strength has been found to be positively correlated with the shape
¹⁶⁶ and size of the clast, for the fabric analysis we subset samples of remains with length
¹⁶⁷ ≥ 2 cm and elongation index (the ratio length/width) $I_e \geq 1.6$ (Lenoble and Bertran,
¹⁶⁸ 2004). The samples are listed in Table 1 and include mostly wood fragments and faunal
¹⁶⁹ remains from the four stratigraphic units under investigation. No distinction of skeletal
¹⁷⁰ elements was made, both due to the high fragmentation rate of faunal remains in Area
¹⁷¹ B, and because recent experiments showed a similar orientation pattern for different
¹⁷² bone shapes (Domínguez-Rodrigo and García-Pérez, 2013; Domínguez-Rodrigo et al.,
¹⁷³ 2012).

Table 1: List of sampled observations for the fabric analysis.

Sample	<i>n</i>	Type		
		Fauna	Wood	Lithic
UA3c	49	23	25	1
UA4	38	8	30	-
<i>E. (P.) antiquus</i>	63			
UB4c (clock)	86	68	4	14
UB4c (compass)	65	47	10	8

174 The sample of bones belonging to the individual of *Elephas (P.) antiquus* from
 175 Area A was analysed separately and included the humerus, ulna, femur and tibia; the
 176 atlas, axis and 16 complete vertebrae or vertebral fragments; 29 complete ribs or rib
 177 fragments; 2 calcanea; 4 metatarsals/metacarpals; the pyramidal; the trapezoid and the
 178 pelvis. The sample from UB5a was too small (only 7 observations) and was therefore
 179 excluded. The sample from the UB4c unit was divided in two sub-samples consid-
 180 ered separately: those recorded using the clock method and those recorded using the
 181 compass method. All the sampled observations are representative of the whole study
 182 area.

183 Rose diagrams and uniformity tests, such as Rayleigh, Kuiper, Watson and Rao
 184 tests ([Jammalamadaka et al., 2001](#)), were used to visualise and evaluate circular isotropy
 185 in the sample distribution. The Rayleigh test is used to assess the significance of the
 186 sample mean resultant length (\bar{R}), assuming that the distribution is unimodal and not
 187 bi- or plurimodal. The \bar{R} ranges from 0 to 1: values close to 1 indicate that the data are
 188 closely clustered around the mean direction; when the data are evenly spread \bar{R} has a
 189 value close to 0. A p -value lower than 0.05 rejects the hypothesis of randomness with
 190 a 95% confidence interval. Kuiper, Watson and Rao are omnibus tests used to detect
 191 multimodal departures from circular uniformity. All of them were applied using a sig-
 192 nificance level of $\alpha = 0.01$. The test results were evaluated against critical values:
 193 a result higher than the critical value rejects the null hypothesis of isotropy with a 99%
 194 confidence interval.

195 Randomness testing of three-dimensional data was conducted with the Woodcock

196 S_1/S_3 test (Woodcock and Naylor, 1983). Considering both the dip (plunge) and strike
197 (bearing) of the oriented items, this method, based on three ordered eigenvalues (S_1 ,
198 S_2 , S_3), is able to discriminate the shape and strength of the distributions. The shape
199 parameter $K = \frac{\ln(S_1/S_2)}{\ln(S_2/S_3)}$ ranges from zero (uni-axial girdles) to infinite (uni-axial clus-
200 ters). The parameter $C = \ln(S_1/S_3)$ expresses the strength of the preferential orien-
201 tation, and its significance is evaluated against critical values from simulated random
202 samples of different sizes. A perfect random uniform distribution would have $C = 0$
203 and $K = 1$.

204 The Benn (Benn, 1994) diagram adds to the Woodcock test an isotropy ($IS =$
205 S_3/S_1) and an elongation ($ES = 1 - (S_2/S_1)$) index. Like the former method, it is
206 able to differentiate between linear (cluster), planar (girdle) or isotropic distributions.
207 There are no published raw data from actualistic studies on depositional processes af-
208 fecting the orientation of bones and artefacts deposited on lacustrine floodplains (but
209 see Morton (2004) and Cobo-Sánchez et al. (2014) as pioneer studies on this subject).
210 However, we included in the Benn diagram references to published results from obser-
211 vation of fabrics in modern subaereal slope deposits (Bertran et al., 1997; Lenoble and
212 Bertran, 2004).

213 Fabric analysis is a powerful tool but, as suggested by Lenoble and Bertran (2004),
214 it is not sufficient to unequivocally discriminate processes and should therefore be in-
215 tegrated with the analysis of other diagnostic features.

216 *2.2. Vertical distribution*

217 The vertical distribution of materials, on the other hand, has been long investi-
218 gated with the aim of identifying cultural levels, by visually interpreting virtual pro-
219 files. Despite recent advances in GIS techniques allow to inspect at higher resolution
220 the three-dimensional distributions of archaeological remains, quantitative approach
221 are still , but see Anderson and Burke (2008). However, archaeological horizons may
222 be subject to vertical rearrangement by syn- and post-depositional processes. Several
223 experimental studies, for example, have investigated the effect of trampling on the ver-
224 tical displacement of artefacts (Villa and Courtin, 1983; Gifford-Gonzalez et al., 1985;
225 Nielsen, 1991; Eren et al., 2010). Although these works have reported a negative cor-

Table 2: List of sampled observations for the vertical distribution and point pattern analyses.

Sample	<i>n</i>	Lithic class					Faunal class			
		Debris/chip	Flake	Bone flake	Tool	Core	Indet.	Bone	Tooth	Microfauna
UA3c	279	46	2	-	1	-	1	171	14	44
UA4	61	3	1	-	-	-	-	45	4	8
UB4c	1243	753	154	1	34	6	2	246	28	19
UB5a	101	50	12	-	3	-	-	30	3	3

226 relation between artefact size and vertical displacement, particle size sorting of lithic
 227 assemblages, when exposed to physical geomorphic agents (such as gravity, water flow,
 228 waves and tides, wind), has been widely documented ([Rick, 1976](#); [Schick, 1986](#); [Pe-](#)
 229 [traglia and Nash, 1987](#); [Morton, 2004](#); [Lenoble, 2005](#); [Bertran et al., 2012](#)).

230 We provisionally assume that a general concentration of unsorted material in the
 231 proximity of the erosional surfaces would support an autochthonous origin of the as-
 232 semblages ; whereas a poorly to extremely poorly sorted and homogeneous vertical dis-
 233 tribution of remains from the UA3c and UB4c units would suggest an allochthonous
 234 origin and a subsequent redeposition triggered by a massive process, e.g., debris or
 235 hyperconcentrated flows. Graded bedding could result in such fluid depositional envi-
 236 ronments, associated with a decrease in transport energy.

237 In order to estimate the degree of vertical dispersion while controlling for the size
 238 of the archaeological material, dimensional classes were set up following typological
 239 criteria. Lithic artefacts were classified as debris/chips when smaller than a cutoff
 240 length of 15 mm (see Tourloukis et al., this issue). Other classes include flakes, tools
 241 and cores; the latter being the bigger and heavier debitage product. Table 2 summarises
 242 the sample size for each class. Lithic debris/chips constitutes the larger part of the
 243 assemblages from UB4c (60%) and UB5a (49%); whereas in Area A it represents only
 244 a moderate percentage in the upper UA3c unit (16%). The very rare presence of lithic
 245 artefacts in the underlying unit UA4 is nevertheless significant. In this unit, the faunal
 246 remains are also found in much lower numbers, their number reduced to one fourth
 247 of those found in UA3c. For the point pattern analysis (see below), we used the same
 248 subset of materials for both excavation areas.

249 For Area B, the material recovered from the water-screening was randomly provenanced
250 according to the 5 cm depth of the excavated spit and the coordinates of the
251 50x50 cm quadrant of the excavation square. Following the same excavation protocol,
252 the same procedure was applied for the water-screened material of Area A, which was
253 randomly provenanced according to 3D-coordinates of the 1x1 m excavation square
254 and 10 cm spit.

255 Inverse-distance weighting (IDW) interpolation of the recorded points of contact
256 between the UB4c/5a and UA3c/4 stratigraphic units were used to reconstruct their
257 erosional surfaces, in Areas A and B, respectively (Fig. 3a,b). IDW assumes spatial
258 autocorrelation and calculates, from a set of irregular known points, weighted average
259 values of unknown points. Thus, in order to address our specific objective, i.e., to
260 quantify and analyse the vertical distribution of the archaeological and palaeontological
261 material, we measured the minimum orthogonal distance of each specimen to the
262 interpolated erosional surface (Fig. 3c).

263 For the units above and below this surface (i.e., UB4c and UB5a), the relative
264 distribution of lithic classes and faunal remains was informally tested by means of
265 kernel density estimations. Likewise, in Area A the relative vertical distribution of
266 remains from UA3c was estimated relative to the absolute elevation of the elephant
267 remains and the range of elevations of the UA3c/4 surface. Finally, a Student's two
268 sample t-test allowed us to compare the empirical distributions of different groups of
269 remains for each stratigraphic unit.

270 *2.3. Point pattern analysis*

271 A spatial point pattern is defined as the outcome of a random spatial point process
272 (repetitions of it would always create a different pattern). The observed patterns of the
273 archaeological and palaeontological remains were treated as manifestations of spatial
274 point processes, i.e., site formation processes. Point pattern analysis investigates the
275 spatial arrangement of points with the aim of identifying spatial trends. In order to
276 integrate the previous studies of the fabric and vertical distributions, we directed our
277 point pattern analysis equally to the intensity of the patterns (the rate of occurrence of
278 the recorded finds) and to the spatial interaction between different types of finds.

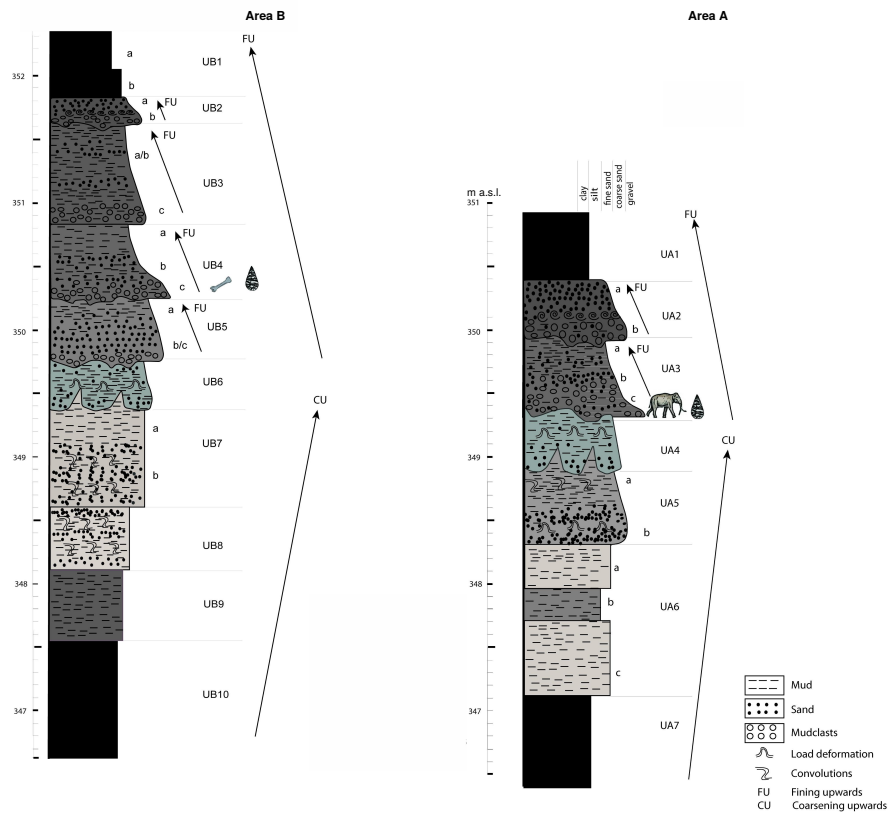


Figure 3: IDW interpolation of the UA3c/4 (a) and UB4c/5a (b) points of erosional contact; the color scale denotes elevation a.s.l. Illustration of the method used to quantify the vertical dispersion of remains with respect to the UB4c/5a surface (c).

279 As the average number of random points per unit area, intensity informs about ho-
280 mogeneity or inhomogeneity in the distribution of events generated by a point process,
281 i.e., whether the rate of occurrence is uniform or spatially varying across the study area.
282 Intensity, usually non-parametrically evaluated by means of kernel density estimation
283 ([Diggle, 1985](#)), was assessed for the distribution of material from the UB4c, UB5a
284 and UA3c units. Cross-validation bandwidth, which assumes a Cox process, and edge
285 correction were applied using the methods described in [Diggle \(1985\)](#).

286 In the presence of a covariate, it is recommended to further investigate the depen-
287 dence of intensity on that explanatory variable. In order to evaluate whether variation
288 in the density of materials was correlated to the topography of the erosional surface,
289 we computed a local likelihood smoothing estimate of the intensity of remains from
290 UB4c as a function of the UB4c/5a surface elevation model ([Baddeley et al., 2012](#)).
291 Formal tests enabled us to assess the evidence of that dependence and to quantify the
292 strength of the covariate. The Kolmogorov-Smirnov test of CSR (Complete Spatial
293 Randomness) and Berman's Z_2 statistics were used to test the strength of evidence for
294 a covariate effect. The Receiver Operating Characteristic (ROC) plot, and the area
295 under the ROC curve (AUC), closely related to Berman's Z_2 test, measure the magni-
296 tude of the covariate effect. AUC values close to 1 or 0 indicate strong discrimination,
297 whereas intermediate values (0.5) suggest no discrimination power.

298 Whereas intensity is a first-order property of the point process, multiscale inter-
299 point interaction is measured by second or higher-order moment quantities, such as
300 the Ripley's K correlation function ([Ripley, 1976, 1977](#)) and the distance G -, F - and
301 J -functions. Three different types of inter-point interaction are possible: random, reg-
302 ular or cluster. Regular patterns are assumed to be the result of inhibition processes,
303 while cluster patterns are the result of attraction processes. In order to reduce the
304 edge effect bias in estimating the correlation between points, we implemented Rip-
305 ley's isotropic edge correction ([Ohser, 1983; Ripley, 1988](#)). In a hypothesis-testing
306 framework, pointwise envelopes were computed by 199 random simulations of the
307 null hypothesis. Thus, values of the empirical distribution (black solid line) were plot-
308 ted against the benchmark value (red dotted line) and the envelopes (grey area) which
309 specify the critical points for a Monte Carlo test ([Ripley, 1981](#)).

310 In order to test the spatial dependence between remains associated with the ero-
311 sional event of UB4c and those associated with the underlying UB5a unit, we treated
312 the data as a multivariate point pattern, assuming that the point patterns in UB4c and
313 UB5a are expressions of two different stationary point processes, i.e., depositional
314 events. We performed a cross-type pair correlation function ($g_{ij}(r)$), derivative of the
315 multitype $K_{ij}(r)$ function, which is the expected number of points of type j lying at a
316 distance r of a typical point of type i . The function is a multiscale measurement of the
317 spatial dependence between types i (UB4c) and j (UB5a). Randomly shifting each of
318 the two patterns, independently of each other, estimated values of $\hat{g}_{ij}(r)$ are compared
319 to a benchmark value $g_{ij}(r) = 1$, which is consistent with independence or at least with
320 lack of correlation between the two point processes.

321 In addition to the pair correlation function, the multitype nearest-neighbour $G_{ij}(r)$
322 function was used to estimate the cumulative distribution of the distance from a point of
323 type i (UB4c) to the nearest point of type j (UB5a). It measures the spatial association
324 between the two assemblages. For the cross-type G -function, the null hypothesis states
325 that the points of type j follow a Poisson (random) distribution in addition to being
326 independent of the points of type i . Thus, in a randomisation technique, when the solid
327 line of the observed distribution ($\hat{G}_{ij}(r)$) is above or below the shaded grey area, the
328 pattern is significantly consistent with clustering or segregation, respectively. Complete
329 spatial randomness and independence (CSRI) of the two point processes would support
330 an exogenous origin hypothesis for the assemblage recovered from the UB4c unit. On
331 the other hand, positive or negative association can be interpreted as expression of
332 different endogenous processes.

333 The particle size spatial distribution of the lithic assemblage from UB4c was inves-
334 tigated by means of a transformation of the multitype K -function ($K_{i\bullet}(r) - K(r)$, see
335 [Baddeley et al. \(2015\)](#), p.608). In this case, we treated the data as the manifestation of a
336 single multitype point process. In a joint distribution analysis, the locations and types
337 of points are assumed to be generated at the same time. The null model of a random
338 labelling test states that the type of each point is determined at random, independently
339 of other points, with fixed probabilities. The estimated K -function for a subset of pos-
340 sible combinations was evaluated against the envelope of Monte Carlo permutations of

341 the class of remains. Likewise with the vertical distribution, a horizontal clustering of
342 small specimens, such as lithic debris/chips, together with larger dimensional classes
343 of remains would suggest the lack of sorting by natural depositional processes and a *en*
344 *mass* model of deposition.

345 As for the three-dimensional distribution of the lithic artefacts in Area A, and their
346 spatial association with the partial skeleton of the *E. (P.) antiquus*, we applied three-
347 dimensional univariate and bivariate second-order functions. A rectangular box of 20
348 square meters and 80 cm vertical extent was selected for the analyses (green outline in
349 Fig. 9a). Assuming homogeneity, the univariate pair correlation function ($g_3(r)$) was
350 estimated for the pattern of all the artefacts (mostly debris/chips) from UA3c and UA4.
351 In the specific context of the site, complete spatial randomness (CSR) would suggest
352 that the pattern most probably is the result of a random distribution process, such as
353 a high energy mass movement. In contrast, other natural processes would produce
354 clustering or segregation of the lithic artefacts. Spatial aggregation, if not generated by
355 obstructions, would support an *in situ* primary origin of the assemblage.

356 In support to the pair correlation function, the cross-type nearest-neighbour func-
357 tion has been applied in order to compute, for each artefact recovered from the UA3c
358 and UA4 units, the nearest point associated with the elephant skeleton. A prevalence
359 of short distances would indicate aggregation of the lithic artefacts around the mass
360 of the elephant; whereas a uniform or symmetric distribution would support random
361 independent processes.

362 3. Results

363 3.1. Fabric analysis

364 The rose diagrams in Fig. 4 visualise the circular distributions of the examined
365 specimens. Overall, the UA4 sample and the sample of elephant bones show predomi-
366 nant peaks in the NE quadrant; while the ones from units UA3c and UB4c suggest uni-
367 form to multimodal distributions. Specifically, the UA4 sample distribution (Fig. 4b)
368 spreads largely in the NE quadrant. Similarly, the circular distribution of the elephant
369 sample (Fig. 4c), mainly lying in UA4, resembles the former distribution: it is skewed

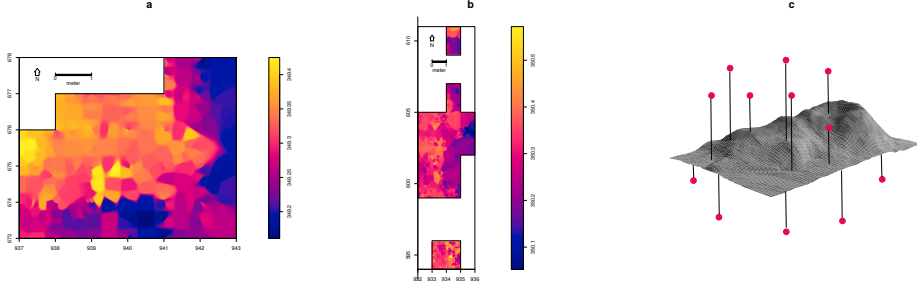


Figure 4: Rose diagrams showing the bearing patterns of samples from UA3c (a), UA4 (b), the elephant carcass (c) and UB4c (d: clock method, e: compass method)

Table 3: Global tests for circular uniformity

Sample	mean dir.	Rayleigh		Kuiper		Watson		Rao		level
		\bar{R}	p - value	test	critical value	test	critical value	test	critical value	
UA3c	77.17°	0.268	0.029	2.4698	2.001	0.2967	0.267	271.8367	160.53	0.01
UA4	35.79°	0.386	0.003	2.5656	2.001	0.3437	0.267	246.3158	163.73	0.01
<i>E. (P.) antiquus</i>	54.64°	0.489	2.775e-07	3.4811	2.001	0.906	0.267	291.4286	155.49	0.01
UB4c (clock)	83.96°	0.167	0.091	2.327	2.001	0.2466	0.267	309.7674	155.49	0.01
UB4c (compass)	128.14°	0.225	0.037	1.6917	2.001	0.1862	0.267	153.3846	155.49	0.01

to the SW and concentrated in the NE quadrant. On the other hand, the UA3c sample (Fig. 4a) and the two samples from Area B (Fig. 4d,e) suggest a different isotropic scenario.

Table 3 summarises the results of the circular uniformity tests. With regard to the UA3c sample, the Rayleigh test ($p - \text{value} = 0.029$) rejected the null hypothesis of circular uniformity. The mean resultant length ($\bar{R} = 0.268$) and the mean direction of 77.17° are thus significant, assuming the distribution is unimodal. However, the Kuiper, Watson and Rao omnibus tests also rejected the null hypothesis of uniformity, therefore suggesting multimodal anisotropy in the distribution, as shown by the rose diagram (Fig. 4a).

For the UA4 sample and the subset of elephant bones, all the tests agreed in rejecting the null hypothesis in favour of a preferentially oriented distribution. The Elephant sample, with respect to the other, showed stronger anisotropy and significantly higher \bar{R} . As suggested by the rose diagrams (Fig. 4c), this sample has a mean direction towards the NE (55°) and relatively low circular variance (29°).

385 The UB4c sub-samples had discordant test results when considering the Rayleigh
386 and the omnibus statistics. According to the Rayleigh test, the mean resultant length
387 (\bar{R}) and the mean direction were not significant for the sub-sample of measurements
388 recorded with the clock system. Conversely, a weak significant test result was obtained
389 for the sub-sample of measurements recorded using the compass. Overall, for the latter
390 sub-sample all the omnibus tests suggested significant isotropy (Fig. 4e). On the other
391 hand, the Kuiper and Rao tests, suggested a multimodal departure from uniformity for
392 the sample recorded using the clock method (Fig. 4d).

393 The results obtained for the UA3c sample and the UB4c sub-sample recorded using
394 the clock method are most probably due to the shape of those distributions. Indeed, the
395 clock system, being less accurate, tends to produce a less dense distribution, more
396 subject to show a multimodal shape when the distribution is actually uniform (Fig. 4a,
397 d).

398 The Woodcock eigenvalues ratio graph (Fig. 5a) presents the shape (K) and strength
399 (C) of the distributions. Fig. 5b plots confidence levels of Monte-Carlo critical C val-
400 ues, varying for sample sizes. The two samples from Area B, together with the UA3c
401 sample, having low C values, plotted close to the origin of the ratio graph. Thus, they
402 suggest nearly significant randomness. On the other hand, the UA4 and the elephant
403 samples, with higher C values, showed a stronger and significant tendency to orient
404 preferentially. The shape parameter K of the samples varied from $K = 0.7$ for the
405 UB4c sample measured with the compass to $K = 0.1$ for the elephant sample. Overall,
406 all the samples plotted below the average shape value ($K = 1$) between girdles and
407 clusters distributions.

408 The Benn diagram (Fig. 6) resembles the Woodcock ratio graph (Fig. 5a). The
409 samples from units UB4c and UA3c clearly plotted at a distance from the UA4 and the
410 elephant samples. The UB4c sub-sample of measurements recorded with the compass,
411 together with the UA3c sample, plotted in the centre of the ternary graph. As shown
412 above, the UB4c sub-sample of measurements taken using the clock system exhibited
413 more isotropy.

414 Compared to the ranges recorded for modern natural processes (debris flow, runoff,
415 solifluction), the fabric from the UA3c and UB4c units plotted well inside the cluster of

.../artwork/Fig5_.pdf

Figure 5: Woodcock's eigenvalues ratio graph (a) and plot of the Monte-Carlo critical S_1/S_3 test values, for varying sample sizes and confidence levels (b), modified from [Woodcock and Naylor \(1983\)](#).

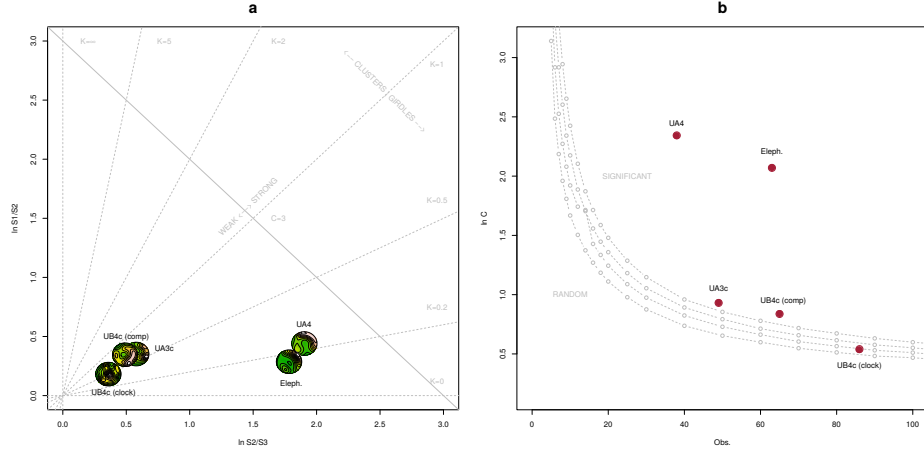


Figure 6: Benn's diagram. Fabric ranges of natural processes modified from Bertran et al. (1997); Lenoble and Bertran (2004).

416 debris flows, with the UB4c (clock) sample suggesting even more random orientations.
 417 On the other hand, the sample of elephant remains, which lie mostly on UA4 and are
 418 covered significantly close to the sample from unit UA4. They both
 419 presented the lowest isotropy index (IS), but not high elongation index (EL). Thus,
 420 they plotted in the average between linear and planar orientations, within the range of
 421 runoff processes. Yet they still plotted at the margins of the cluster of debris flows
 422 fabrics. Moreover, the elephant sample showed a more planar attitude with respect to
 423 the UA4 sample.

424 3.2. Vertical distribution

425 Fig. 7 compares the distribution of the absolute elevations of the partial skeleton
 426 of the *Elephas (P.) antiquus* with the other remains from Area A. Overall, the vertical
 427 distribution of the elephant approximates a normal distribution with mean (μ) 349.25 m
 428 a.s.l. and standard deviation (σ) 0.12 m. The mean elevation of the erosional contact
 429 between the two stratigraphic units is slightly above the latter ($\mu = 349.30$ m). Al-
 430 though difficult to quantify due to its mixed nature, the range of elevations of this con-
 431 tact, as estimated from the IDW interpolation (Fig. 3a), is relatively small ($\sigma = 0.06$ m).

432 Three lithic artefacts (two flakes and one tool) from the UA3c unit are located

433 within its positive half. Only one flake has been found in the lower UA4, at about
434 349.10 m, together with three chips. However, they plotted well within the left tail
435 of the debris/chip distribution from the unit above. Despite the scarcity of debitage
436 products in this area, waste products (debris/chip) are relatively well represented (16%
437 of the UA3c sample). Their vertical distribution approximates a normal distribution
438 ($\mu = 349.50$ m and $\sigma = 0.18$ m), having almost 50% of the sample in the range of
439 elevations of the erosional surface and the rest above it. Notably, the distribution of
440 the faunal remains from the same unit resembles that of the debris/chip. The Welch
441 two sample t-test ($p - value = 0.5099$) failed to reject the null hypothesis that the
442 two population means are equal. On the other hand, the vertical distribution of faunal
443 remains recovered from the UA4 unit is comparable with that of the *Elephas* ($p -$
444 $value = 0.6562$). Nevertheless, the density functions altogether clearly confirm one
445 of the main observations assessed during excavation, namely that the elephant remains
446 and most of the recovered faunal and lithic material in Area A lie at or close to the
447 UA3c/4 contact, with unit UA3c covering the remains.

448 Fig. 8 shows the empirical density functions of the minimum distances from each
449 specimen from Area B to the UB4c/5a erosional contact (Fig. 3b). The combined
450 distribution of any type of find from the UB5a unit (Fig. 8a) skewed to the left with
451 a short tail (up to -0.3 m). The mode, between 5 and 10 cm below the roof of UB5a,
452 indicates a general concentration of material very close to the contact of this unit with
453 the overlying UB4c, in accordance with the mean distribution of the different classes of
454 remains. Although the majority of both the lithic and faunal assemblages were found
455 in the uppermost 15 cm of UB5a, few debris/chips and bone fragments occur lower
456 in the sequence, yet no more than 30 cm below the roof of this unit. Very few flakes,
457 three tools and no cores have been found in this unit. As a whole, the lithic assemblage
458 from UB5a, mostly composed by debris/chips, is only 7% of the most conspicuous
459 assemblage from UB4c.

460 The global distribution of unit UB4c was right skewed (up to almost 0.6 m) and cen-
461 centred at about 5 cm above the contact with the underlying unit UB5a (Fig. 8b). Almost
462 30% of the sample fell exactly at the erosional contact that separates UB4c from UB5a.
463 The density estimations of the lithic debris/chip, flakes, tools and faunal remains sig-

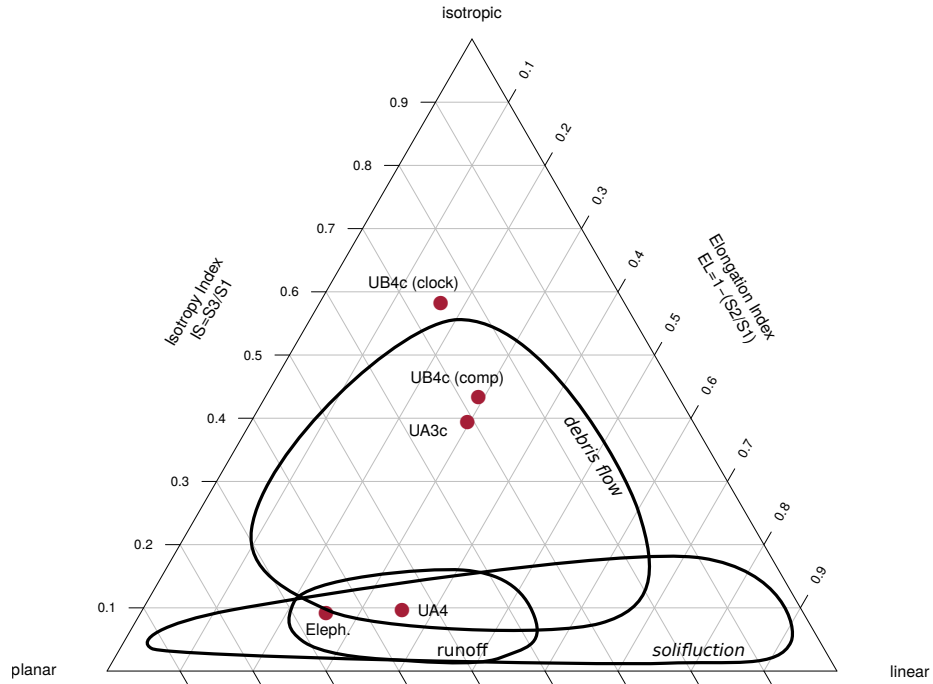


Figure 7: Empirical density functions of absolute elevations (meters a.s.l) of remains from Area A. The histogram represents the *Elephas (P.) antiquus* range of elevations; the grey area shades the $Q_3 - Q_1$ range of the erosional UA3c/4 surface; dashed lines indicate mean values.

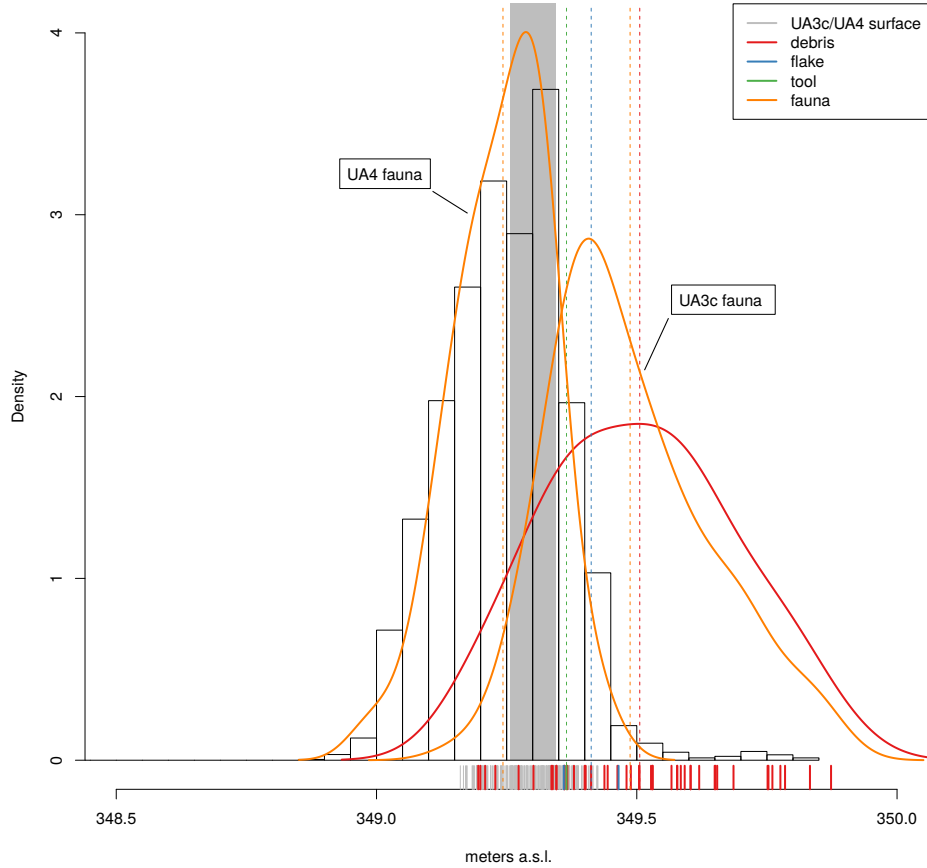


Figure 8: Empirical density functions of minimum orthogonal distances (d) to the UB4c/5a surface. The histogram represents the total distribution of remains from UB5a (a) and UB4c (b); dashed lines indicate mean values.

nificantly overlap, whereas the distribution of the six cores shows a bimodal shape with peaks at 5 and 20 cm above the contact. However, the Welch Two Sample t-test of the lithic and faunal sample means failed to reject the null hypothesis ($p-value = 0.6295$).

3.3. Point pattern analysis

Results of the point pattern analysis are complementary to those obtained from the analysis of the vertical and fabric distributions.

Regarding Area A, kernel density estimation and three-dimensional functions were applied in order to quantitatively depict the spatial distribution of the lithic assemblage

472 in relation to the elephant skeleton.

473 Fig. 9a shows the smoothing kernel intensity estimation of the combined lithic and
474 faunal assemblage from the UA3c unit. Contour lines delimit the density of the lithic
475 sample. The partial skeleton of the *E. (P.) antiquus* is superimposed on it. A pre-
476 liminary visual examination of the plot suggests a homogeneous distribution of lithics
477 (mostly debris/chips) and fossils. Spots of higher density appear to be spread around
478 and in association with the elephant remains.

479 The univariate pair correlation function of the joined lithic assemblage from the
480 UA3c and UA4 units (Fig. 9b) suggests aggregation of finds. The estimated $\hat{g}_3(r)$
481 function (black solid line) wanders above the benchmark value (red dotted line) until
482 values of $r = 0.8$. However, for distances between 35 and 65 cm, it lies above the
483 grey envelope of significance for the null hypothesis of CSR, indicating that at those
484 distances artefacts occur closer than expected in the case of random processes. For
485 values of $r > 0.8$, the function stabilises at values close to 0, suggesting a Poisson
486 distribution. The plot illustrates the random distribution of finds between patches of
487 clusters that we observe in the kernel density estimation (Fig. 9a).

488 The histogram in Fig. 9c shows the density of the distances calculated from each
489 artefact to the nearest-neighbour elephant remain. A right skewed distribution, with
490 a prevalent peak at 10 cm and mean $\mu \approx 30$ cm is an indication of the relatively strong
491 aggregation of events around the mass of the elephant skeleton.

492 As for Area B, the analysis first focused on the spatial distribution and cross-
493 correlation of the assemblages from UB4c and UB5a (Fig. 10); and secondly on the
494 interaction between classes of remains from UB4c (Fig. 11).

495 Figs. 10a,b respectively show kernel density estimations of the combined lithic and
496 faunal assemblages from both the units analysed. Despite the samples size difference,
497 a first visual examination suggests the presence of interesting spatial structures.

498 Regarding the UB4c unit (Fig. 10a), the high density of material concentrated
499 around the western square 934/600 suggests that the pattern could have been the re-
500 sult of an inhomogeneous, non-uniform depositional process. Visual comparison of
501 the density plot with the elevation model of the erosional contact between the UB4c
502 and UB5a units (Fig. 3b) suggests positive correlation between lower elevations (topo-

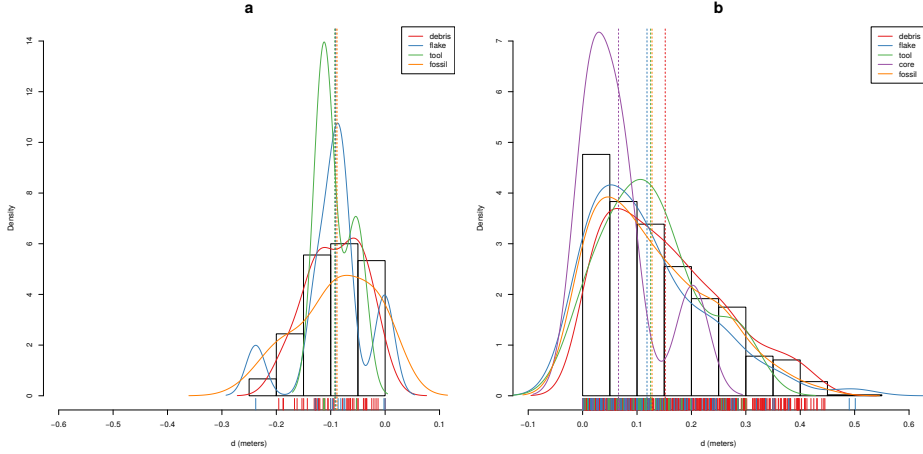


Figure 9: Kernel smoothed intensity function of the lithic and faunal assemblages from UA3c. Isolines mark the density of the lithic artefacts (a). Pair correlation function ($g_3(r)$) of a three-dimensional pattern of lithic artefacts from UA3c and UA4. Grey envelope of 999 Monte Carlo simulations under the CSR null hypothesis (b). Three-dimensional distance from each lithic artefact from UA3c and UA4 to the nearest neighbour elephant remain (c).

graphic depressions) and higher density of remains. Fig. 10c shows the results of the ρ -function, which estimates the intensity of the UB4c sample assemblage as a function of the covariate underlying topography created by the erosional event. Within the range of elevation between 350.2 and 350.4 m, the occurrence of finds is higher and the intensity decreases with the rise of elevation, i.e., finds are more likely to be found at lower elevations than would be expected if the intensity was constant.

Spatial Kolmogorov-Smirnov and Berman's Z_2 (Berman, 1986) statistics were used in order to test the dependence of the UB4c pattern on the covariate erosional surface. Both KS ($D = 0.11952$, $p - value = 7.772e - 16$) and Z_2 ($Z2 = -7.8447$, $p - value = 4.34e - 15$) significantly rejected the null hypothesis of CSR. Although the tests suggested evidence that the intensity depends on the covariate, the effect of the covariate is weak and it seems to have no discriminatory power. The ROC curve and AUC statistics (0.56), which measure the strength of the covariate effect, suggest that the underlying UB4c/5a topography does not completely explain the localised high density of occurrence in the UB4c.

518 Relative spatial segregation seems to occur between the assemblages from UB4c
519 (Fig. 10a) and UB5a (Fig. 10b), with high density of the former distribution corre-
520 sponding to low density of the latter. The former analysis of the vertical distribution
521 showed that the two assemblages occur very close to their stratigraphic contact. In
522 order to further investigate the spatial interaction between the two depositional events,
523 we applied multitype pair correlation ($g_{ij}(r)$) and nearest-neighbour ($G_{ij}(r)$) functions.

524 Fig. 10d shows the estimated values of the multivariate $\hat{g}_{ij}(r)$ function against the
525 envelope of the null hypothesis, obtained by randomly shifting the position of remains
526 from the two distributions in 199 Monte Carlo simulations. For fixed values of r less
527 than 30 cm the observed function lies below the benchmark value of independence, thus
528 indicating segregation; but it wanders at the lower edge of the grey envelope. For fixed
529 distances of $r > 0.3$ m the observed and theoretical lines significantly overlap. Overall,
530 the function suggests independence of the two point processes (UB4c and UB5a) at
531 multiple scales.

532 However, the estimated $\hat{G}_{ij}(r)$ function (Fig. 10c), running well below the signifi-
533 cance grey envelope for fixed values of $r > 0.3$ m, confirms that the nearest-neighbour
534 distances between remains from UB4c and UB5a are significantly longer than expected
535 in the case of independent processes. Interestingly, at values of $r < 0.2$ m the observed
536 function failed to reject the null hypothesis of Complete Spatial Randomness and In-
537 dependence (CSRI).

538 With the aim to integrate the vertical distribution analysis, the particle size spatial
539 distribution of remains from the UB4c unit were investigated by means of a deriva-
540 tive of the multitype K -function, randomly labelling the classes of remains. Fig.11
541 shows a selection of the array of possible combinations between classes. In any panel,
542 the estimated function wanders above the benchmark value. Such positive deviations
543 from the null hypotheses suggest that debris/chips are more likely to be found close
544 to the other class of remains than would be expected in case of a completely random
545 distribution. Permutating the lithic debris/chips with flakes (Fig.11a), tools (Fig.11b),
546 cores (Fig.11c) and faunal remains (Fig.11d), the Monte Carlo test results would have
547 been significantly consistent with clustering, if we had chosen distance values $r > 0.4$,
548 $r > 0.4$, $r > 0.9$, $r > 0.8$, respectively. Conversely, we could not reject the null

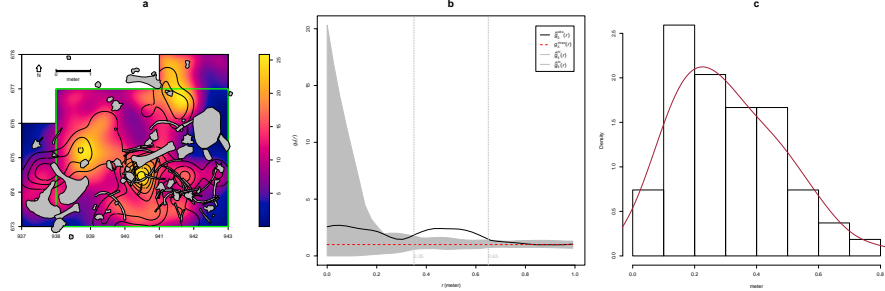


Figure 10: Kernel smoothed intensity function of the lithic and faunal assemblages from UB4c (a) and UB5a (b). Smoothing estimate of the intensity of remains from UB4c, as a function of the erosional surface UB4c/5a. Grey shading is pointwise 95% confidence bands (c). Cross-pattern pair correlation function ($g_{ij}(r)$) between the UB4c and UB5a distributions. Grey envelope of 199 Monte Carlo simulations under the independence of components null hypothesis (d). Multitype nearest-neighbour function ($G_{ij}(r)$) between the UB4c and UB5a distributions (e).

549 hypothesis of CSRI for lesser values of r .

550 4. Discussion

551 Recent excavations at the Middle Pleistocene site of Marathousa 1 have unearthed
 552 in one of the two investigated areas (Area A) a partial skeleton of a single individual of
 553 *Elephas (P.) antiquus*, whose bones are in close anatomical association, and spatially
 554 and stratigraphically associated with lithic artefacts and other faunal remains. In Area
 555 B, 60 m to the South of Area A, we collected a much higher number of lithic artefacts
 556 (Tourloukis et al., this issue), spatially and stratigraphically associated with other fau-
 557 nal remains, including isolated elephant bones, cervids and carnivores among others
 558 (Konidaris et al., this issue).

559 The two areas are stratigraphically correlated, the main fossiliferous layers (UA3c
 560 and UB4c) representing a relatively low-energy depositional process, such as a hyper-
 561 concentrated flow that dumped material in a lake margin context (Karkanas et al., this
 562 issue).

563 To date, evidence of butchering (cut-marks) has been identified on two bones of
 564 the elephant skeleton from Area A, as well on elephant and other mammal bones from

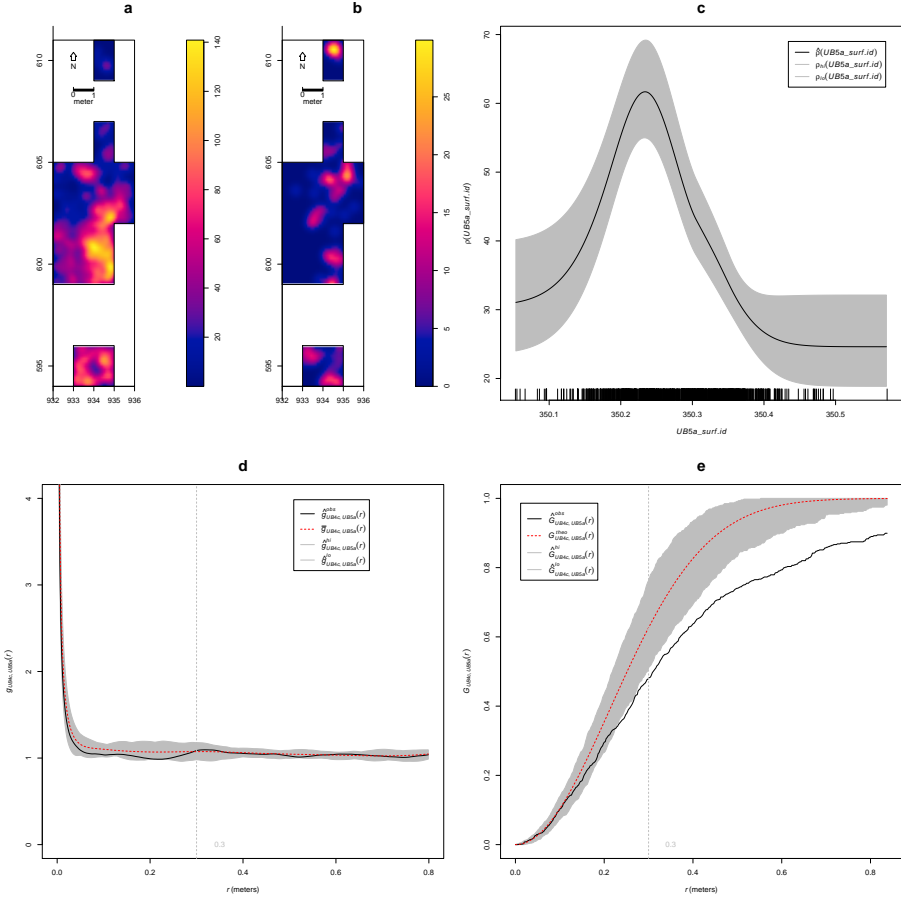


Figure 11: Random labelling test for the UB4c assemblage. Grey pointwise envelope of 199 Monte Carlo permutation of debris/chips with flakes (a); tools (b); cores (c); flakes/tools (d); fossils (e).

565 Area B (see Konidaris, this issue).

566 However, due to the secondary depositional nature of the main fossiliferous hori-
567 zon, it is of primary importance to evaluate the degree and reliability of the spatial
568 association of the lithic artefacts with the faunal remains, and especially with the ele-
569 phant skeleton. In order to tackle our main objective, we applied a comprehensive
570 set of spatial statistics to the distributions of the archaeological and zooarchaeologi-
571 cal/palaeontological remains from relevant stratigraphic units of the two areas of in-
572 vestigation. Results of our analyses are here discussed for both areas.

573 *4.1. Fabric analysis*

574 The analysis of the orientation (dip and strike) of subsets of remains, mostly bone
575 fragments, organic residues and lithic artefacts, showed different patterns for the two
576 main find-bearing units.

577 The test results (Tab. 3) for the UA4 sample and the sample of elephant remains
578 - which lie on unit UA4 and are covered by UA3c - indicated significant preferential
579 orientations towards the NE (Figs. 4b,c). As shown by the Woodcock's (Fig. 5) and the
580 Benn's diagrams (Fig. 6), these samples plotted together at a distance from the others.
581 Such convergence suggests that the elephant carcass, the other faunal remains and the
582 organic material, deposited on unit UA4, were subject to the same processes.

583 Far from the isotropic corner in the Benn's diagram these two samples from Area
584 A plotted approximately in between the linear and planar extremes, with the elephant
585 sample showing a more planar fabric. When the results published by Bertran et al.
586 (1997) and Lenoble and Bertran (2004) from observations of fabrics in modern sub-
587 aereal slope deposits were used as a reference, the two samples aggregated well within
588 the cluster of runoff process. Yet, they still plotted at the extreme margins of debris
589 flow and relatively distant from the linear corner.

590 This result is consistent with the exposure of unit UA4 to overland water-laden
591 processes that occurred before the flood event UA3/UB4 (Karkanas et al., this is-
592 sue). Notably, the erosive nature of low-energy processes triggered by rain-water has
593 been observed on lacustrine floodplains, and is associated with anisotropic patterns
594 in autochthonous assemblages (Cobo-Sánchez et al., 2014; Domínguez-Rodrigo et al.,

595 2014c; García-Moreno et al., 2016).

596 On the other hand, the fabric of the UA3c sample, being similar to those of the
597 UB4c sub-samples (Figs. 5 and 6), supports the stratigraphic correlation between these
598 units across the two investigated areas. The fabric analysis suggests that the UA3/UB4
599 process can be categorized as a flood event, which falls in between the spectrum of de-
600 bris and hyperconcentrated flow. Indeed, random distribution and orientation of clasts
601 is expected for debris flows, except at flow margins, where preferential orientation and
602 clusters of clasts have been observed (Pierson, 2005).

603 Unlike bones with a tubular shape (i.e., long bones), ribs and vertebrae are prone
604 to orient preferentially under high energy processes, less likely under low energy pro-
605 cesses (Domínguez-Rodrigo and García-Pérez, 2013; Domínguez-Rodrigo et al., 2014c).
606 Interestingly, whereas some of the ribs share the same preferential orientation with the
607 long bones, others are oriented NW/SE. However, a NW/SE orientation could be con-
608 sistent with a prevalent NE direction of the flow (and vice-versa), since long bones
609 could roll orthogonally to the flow direction (Voorhies, 1966).

610 On the other hand, a higher energy flood would lead to an under-representation
611 of most cancellous grease-bearing bones, which are prone to be easily transported by
612 water induced processes (Voorhies, 1966). Yet several carpals, tarsals, metapodials,
613 phalanges, ribs and vertebrae are present and in close spatial association with the ele-
614 phant cranium and other skeletal elements.

615 The presence of many of the skeletal elements suggests that the elephant carcass
616 was not subjected to high energy processes. Thus, we can assume that relatively low
617 energy overland flows slightly reworked and oriented the exposed elements of the
618 already dismembered (and probably already marginally displaced) elephant carcass,
619 which mostly preserves close anatomical associations, but not anatomical connections.

620 In Area B, two sub-samples from the same stratigraphic unit were analysed, accord-
621 ing to the different methods used for recording the orientation (dip and strike) of the
622 finds (i.e., 'clock' vs. compass), mostly faunal remains, wood fragments and lithic arte-
623 facts. Due to the different shapes of the two distributions (Figs. 4d,e), test statistics re-
624 ported contrasting results (Tab. 3). Indeed, the clock system, recording non-continuous
625 circular data, tends to produce a distribution more subject to show a multimodal shape

when the distribution is actually uniform. However, the three-dimensional Woodcock (Fig. 5) and Benn (Fig. 6) diagrams agreed upon assessing the randomness of the samples. Despite minor differences between the two samples, both plotted with the UA3c sample in the reference range of debris flows.

4.2. Vertical distribution

As for the vertical distribution, we assume that mass wasting processes, such as debris or hyperconcentrated flows, would predominantly distribute extremely poorly sorted clasts homogeneously throughout the sequence. Normal or inverse grading can be observed in such flows (Pierson, 2005). A concentration of unsorted elements in the proximity of the erosional surface, as well as the absence of any grading, would in turn suggest an autochthonous assemblage.

The lithic assemblage from Area A - the combined sample from units UA3c and UA4 ($n = 54$), composed by a few debitage products and a relatively high number of debris/chips and retouch waste products (Tab. 2) - plotted predominantly in the proximity of the erosional surface created by the UA3/UB4 event. The faunal remains from unit UA3c resemble the distribution of the archaeological assemblage as a whole; whereas the ones from the underlying unit UA4 match the vertical distribution of the elephant (Fig. 7).

Overall, the material recovered from unit UA3c did not show any grading and mainly plotted at the bottom of the unit, thus is consistent with the hypothesis of an autochthonous assemblage.

In Area B, two samples from units UB4c ($n = 1243$) and UB5a ($n = 101$) respectively, were analysed (Tab. 2) for quantifying the minimum orthogonal distance of each item to the modelled erosional surface (Fig. 3b).

The vertical distribution of lithic artefacts and fossils from unit UB4c showed a predominant peak right at the contact with the erosional surface. Almost 30% of this rich sample plotted at a distance between 0 and 5 cm from the erosional contact; whereas the rest gently skewed to the upper part of the unit, up to about 50 cm. The same distribution was observed for all classes of remains, suggesting no size sorting and an origin very close to the erosional surface (Fig. 8b).

656 The density distribution of the sample from the underlying UB5a unit (Fig. 8a)
657 globally indicates a more constrained vertical displacement of remains (within 30 cm
658 below the erosional surface). Whereas lithic artefacts and fossils mostly plot right at
659 the contact and just below it, a few debris/chips and faunal remains were found lower
660 in the sequence. No size sorting was observed, but, notably, lithic cores are absent and
661 the debris/chip distribution is wider than the distribution of the few flakes and tools.

662 Field observations of cracks in the clayey UB5a unit testify to shrinking and swelling
663 during wet and dry cycles (Karkanas et al., this issue), which suggests that vertical dis-
664 placement of some small lithics and fossil fragments at lower depths with respect to
665 the UB5a/4c contact probably resulted from clay desiccation.

666 Likewise, [Lenoble and Bertran \(2004\)](#) documented up to 30 cm vertical dispersion
667 and frequent vertical dip of artefacts from the marshy silty clay of the Croix-de-Canard
668 site, sector 3.

669 Furthermore, a recent experimental study of animal trampling in water saturated
670 substrates reported negative correlation with artefact size, significant inclination and
671 greater vertical displacement than any former work: a maximum between 16 and
672 21 cm, with a mean of about 6 cm ([Eren et al., 2010](#)).

673 The fact that the majority of the remains from units UB4c and UB5a plotted at,
674 or very close to the contact between these two layers, the relatively high percentage
675 of lithics in both units, as well as the absence of size sorting or grading, suggest au-
676 tochthonous assemblages, deposited in UB5a and subsequently eroded *in situ* by the
677 UA3/UB4 flood event.

678 *4.3. Point pattern analysis*

679 The hypothesis that in both areas the lithic and faunal assemblages were primarily
680 deposited *in situ* and were subsequently reworked by a low energy flood, was further
681 explored by means of point pattern analysis.

682 We assumed that a completely random spatial distribution of the lithic artefacts
683 and faunal remains would suggest an allochthonous origin and subsequent transport to
684 the site by the action of a random massive process, such as debris flow. Nevertheless,
685 clustering of artefacts is not necessarily evidence of human presence. Aggregation or

686 segregation patterns could be produced by a range of biotic and/or natural processes.
687 Human activities, topography and physical obstructions alike could trigger spatial ag-
688 gregation.

689 The three-dimensional distribution of lithic artefacts from unit UA3c shows signif-
690 icant clustering for values of r between 35 and 65 cm. Lithic artefacts occur relatively
691 close to the skeletal elements of the elephant, at a distance between 20 and 50 cm at
692 most (Fig. 9). The richest cluster of about 20 lithic artefacts is located to the SW of the
693 cranium, close to the right femur and the scatter of ribs and vertebrae.

694 Considering the prevalent NE orientation of the elephant bones and the other fau-
695 nal remains from UA4, it is not unlikely that a SW/NE oriented flood could have been
696 responsible for the observed accumulation to the SW of the elephant cranium, which
697 would have represented an important obstruction to the flow. A similar case of clus-
698 tering of small remains, apparently dammed by a long elephant tusk, has also been
699 observed at Castel di Guido (Italy) ([Boschian and Saccà, 2010](#)). Secondary deposi-
700 tion by low-energy flows and clustering of artefacts and bones blocked by an aurochs
701 carcass have been as well documented at the site of 'Ein Qashishadd (Israel) (?).

702 As mentioned above, whereas fairly random fabric and spatial distribution of coarse
703 clasts are observed at the centre of modern debris flow deposits, preferential orientation
704 and clustering may occur at the margin of the flood ([Pierson, 2005](#)). Yet the fabric
705 analysis of the UA3c sample shows a random distribution, which falls within the range
706 of debris flow (Fig. 6), and the pair correlation function (Fig. 9b) suggests significant
707 clustering of lithic artefacts at relatively small scale: a pattern less likely to be produced
708 by a large scale massive process such as a debris flow. Moreover, clusters of lithic
709 artefacts occur as well in areas with lower densities of elephant bones.

710 Small scale clustering; proximity to the elephant remains and the erosional surface;
711 absence of spatial size sorting and, on the contrary, the presence of a relatively high
712 number of lithic debris/chips associated with some flakes and tools; close anatomical
713 spatial association of the elephant skeletal elements, slightly displaced and preferen-
714 tially oriented: these lines of evidences support the hypothesis of an autochthonous
715 deposition, subject to localised minor reworking.

716 A similar pattern can be observed in Area B, where an initial set of spatial statistics

717 confirmed that the inhomogeneous density of remains from unit UB4c (Fig. 10a) is
718 not completely explained by the covariate effect of the underlying complex topography
719 created by the erosional event UA3/UB4 (Fig. 3b).

720 Thus, we explored the relative spatial interaction between the UB4c and the un-
721 derlying UB5a samples. We assumed that complete spatial randomness of the two
722 independent depositional processes would occur in case of an exogenous origin and
723 transportation of the UB4c assemblage. The hypothesis of an autochthonous original
724 deposition of the faunal and lithic assemblages on the UB5a unit, subsequently eroded
725 *in situ* by a relatively high energy flood (UB4c), was tested by cross-pattern spatial
726 correlation functions (Figs. 10d,e). Whereas the two samples are vertically adjacent to
727 the erosional surface (Fig. 8), on the horizontal plane they are both more segregated
728 than expected for a random distribution.

729 Moreover, for the UB4c sample, an unsorted particle size spatial distribution was
730 confirmed (Fig. 11). The occurrence in the same place of small and large classes of
731 remains suggests that post-depositional processes, such as water winnowing, have not
732 severely affected the assemblage. Hyperconcentrated flows would have dumped mate-
733 rial onto the lake margin. In this way, particles would have been frozen and deposited
734 *en masse*. Hence their non-sorted spatial distribution.

735 Conversely, the extraordinary preservation and number of mint to sharp, unsorted
736 lithic artefacts from the UB4c unit; their density, positively correlated to the topog-
737 raphy, and significantly segregated from the underlying distribution of remains; the
738 vertical proximity of both assemblages from UB4c and UB5a to the erosional surface;
739 as well as the random orientation pattern of the former, suggest that significant dis-
740 placement of materials due to the erosional event can be excluded.

741 The faunal and lithic assemblages from unit UB4c therefore most likely derived
742 from the local erosion of exposed mudflat areas (UB5a layer) and have been slightly
743 redistributed by the same flood event that capped the elephant in Area A.

744 Further evidence that the recovered assemblage has not undergone substantial re-
745 working and has retained its original characteristics would come from the refitting anal-
746 ysis, currently in progress. To date, 4 bone refits have been found in Area B: three from
747 unit UB4c, respectively at 4.77, 0.05 and 0.01 m distance; and one between two mam-

748 mal bone fragments from units UB4c and UB5a, at a very short distance (0.09 m).
749 Interestingly, one of the elements of the most distant refit (a *Dama sp.* mandibular
750 fragment) shows traces of carnivore gnawing (Konidaris et al., this issue).

751 In conclusion, multiple lines of evidence suggest that the erosional event UB4/UA3
752 represents a relatively low-energy process in the continuum between debris and hyper-
753 concentrated flow, which would have locally reworked at a small scale the already
754 exposed or slightly buried and spatially associated lithic and faunal assemblages.

755 Although the UB4/UA3 process represents a snapshot of a relatively short time-
756 frame, inferences about the use of space by human groups, in terms of knapping
757 episodes and butchering activities, are unreliable in light of the current information.

758 The spatial pattern observed at the site is indeed the result of the last episode in
759 a palimpsest of spatial processes. Whereas the erosional event represented by the de-
760 bris/hyperconcentrated flow UA3/UB4 caps the sequence and preserves the record, lit-
761 tle is known about the eroded underlying occupational horizon.

762 However, whereas hunting or scavenging is still an unsolved matter of debate, con-
763 sidering the rate of bone fragmentation, the density of lithic debris/chips, the number
764 of processed bones and their spatial density and association, it is likely that the assem-
765 blage represents a complex palimpsest of locally repeated events of hunting/scavenging
766 and exploitation of lake shore resources.

767 More data from high resolution excavations in the coming years will allow us to
768 refine the coarse-grained spatio-temporal resolution of our inferences about past human
769 behaviour at Marathousa 1.

770 5. Conclusions

771 At the Middle Pleistocene open-air site of Marathousa 1, a partial skeleton of a
772 single individual of *Elephas (Palaeoloxodon) antiquus* was recovered in stratigraphic
773 association with a rich and consistent lithic assemblage and other vertebrate remains.
774 Cut-marks and percussion marks have been identified on the elephant and other mam-
775 mal bones excavated at the site. The main find-bearing horizon represents a secondary
776 depositional process in a lake margin context.

777 Understanding the site formation processes is of primary importance in order to
778 reliably infer hominin exploitation of the elephant carcass and other animals. To meet
779 this aim, we applied a comprehensive set of multivariate and multiscale spatial analyses
780 in a taphonomic framework.

781 Results from the fabric, vertical distribution and point pattern analyses are consis-
782 tent with a relatively low-energy erosional process slightly reworking at a small scale
783 an exposed (or slightly buried) and consistent scatter of lithic artefacts and faunal re-
784 mains. These results are in agreement with preliminary taphonomic observations of
785 the lithic artefacts (Tourloukis et al., this issue) and the faunal remains (Konidaris et
786 al., this issue), which also indicate minor weathering and transportation. Our analyses
787 show that multiple lines of evidence support an autochthonous origin of the lithic and
788 faunal assemblages, subject to minor post-depositional reworking. Human activities
789 therefore took place on-site, during an as of yet uncertain range of time.

790 **Acknowledgements**

791 This research is supported by the European Research Council (ERC StG PaGE
792 283503) awarded to K. Harvati. We are grateful to the Municipality of Megalopolis,
793 the authorities of the Region of Peloponnese, and the Greek Public Power corporation
794 (Δ EH) for their support. We also thank Julian Bega and all the participants in the PaGE
795 survey and excavation campaigns in Megalopolis for their indispensable cooperation.

796 **References**

- 797 Anderson, K. L., Burke, A., 2008. Refining the definition of cultural levels at Karabi
798 Tamchin: a quantitative approach to vertical intra-site spatial analysis. Journal of
799 Archaeological Science 35 (8), 2274–2285.
- 800 Baddeley, A., Chang, Y.-M., Song, Y., Turner, R., 2012. Nonparametric estimation of
801 the dependence of a point process on spatial covariates. Statistics and Its Interface
802 5 (2), 221–236.

- 803 Baddeley, A., Rubak, E., Turner, R., 2015. Spatial Point Patterns: Methodology and
804 Applications with R. Chapman and Hall/CRC, London.
- 805 Bar-Yosef, O., Tchernov, E., 1972. On the palaeo-ecological history of the site of Ubei-
806 diya. Vol. 35. Israel Academy of Sciences and Humanities, Jerusalem.
- 807 Bargalló, A., Gabucio, M. J., Rivals, F., 2016. Puzzling out a palimpsest: Testing
808 an interdisciplinary study in level o of abric romaní. Quaternary International
809 417 (Supplement C), 51 – 65, advances in Palimpsest Dissection.
- 810 URL [http://www.sciencedirect.com/science/article/pii/
811 S1040618215009635](http://www.sciencedirect.com/science/article/pii/S1040618215009635)
- 812 Benito-Calvo, A., de la Torre, I., 2011. Analysis of orientation patterns in Olduvai
813 Bed I assemblages using GIS techniques: Implications for site formation processes.
814 Journal of Human Evolution 61 (1), 50 – 60.
- 815 Benito-Calvo, A., Martínez-Moreno, J., Mora, R., Roy, M., Roda, X., 2011. Trampling
816 experiments at Cova Gran de Santa Linya, Pre-Pyrenees, Spain: their relevance for
817 archaeological fabrics of the Upper–Middle Paleolithic assemblages. Journal of Ar-
818 chaeological Science 38 (12), 3652–3661.
- 819 Benito-Calvo, A., Martínez-Moreno, J., Pardo, J. F. J., de la Torre, I., Torcal, R. M.,
820 2009. Sedimentological and archaeological fabrics in Palaeolithic levels of the
821 South-Eastern Pyrenees: Cova Gran and Roca dels Bous Sites (Lleida, Spain). Jour-
822 nal of Archaeological Science 36 (11), 2566 – 2577.
- 823 Benn, D., 1994. Fabric shape and the interpretation of sedimentary fabric data. Journal
824 of Sedimentary Research 64 (4a), 910–915.
- 825 Berman, M., 1986. Testing for spatial association between a point process and another
826 stochastic process. Applied Statistics 35, 54–62.
- 827 Bernatchez, J. A., 2010. Taphonomic implications of orientation of plotted finds from
828 Pinnacle Point 13B (Mossel Bay, Western Cape Province, South Africa). Journal of
829 Human Evolution 59 (3–4), 274 – 288.

- 830 Bertran, P., Hetù, B., Texier, J.-P., Steijn, H. V., 1997. Fabric characteristics of subaerial
831 slope deposits. *Sedimentology* 44 (1), 1 – 16.
- 832 Bertran, P., Lenoble, A., Todisco, D., Desrosiers, P. M., Sørensen, M., 2012. Particle
833 size distribution of lithic assemblages and taphonomy of Palaeolithic sites. *Journal*
834 of Archaeological Science 39 (10), 3148 – 3166.
- 835 Bertran, P., Texier, J.-P., 1995. Fabric Analysis: Application to Paleolithic Sites. *Jour-*
836 *nal of Archaeological Science* 22 (4), 521 – 535.
- 837 Bevan, A., Crema, E., Li, X., Palmisano, A., 2013. Intensities, Interactions, and Un-
838 certainties: Some New Approaches to Archaeological Distributions. In: Bevan, A.,
839 Lake, M. (Eds.), *Computational Approaches to Archaeological Spaces*. Left Coast
840 Press, Walnut Creek, pp. 27–52.
- 841 Boschian, G., Saccà, D., 2010. Ambiguities in human and elephant interactions? Sto-
842 ries of bones, sand and water from Castel di Guido (Italy). *Quaternary International*
843 214 (1–2), 3 – 16.
- 844 Carrer, F., 2015. Interpreting Intra-site Spatial Patterns in Seasonal Contexts: an Eth-
845 noarchaeological Case Study from the Western Alps. *Journal of Archaeological*
846 *Method and Theory*, 1–25.
- 847 Clark, A. E., 2016. Time and space in the middle paleolithic: Spatial structure and
848 occupation dynamics of seven open-air sites. *Evolutionary Anthropology: Issues,*
849 *News, and Reviews* 25 (3), 153–163.
- 850 Cobo-Sánchez, L., Aramendi, J., Domínguez-Rodrigo, M., 2014. Orientation patterns
851 of wildebeest bones on the lake Masek floodplain (Serengeti, Tanzania) and their
852 relevance to interpret anisotropy in the Olduvai lacustrine floodplain. *Quaternary*
853 *International* 322–323 (0), 277 – 284.
- 854 de la Torre, I., Benito-Calvo, A., 2013. Application of GIS methods to retrieve ori-
855 entation patterns from imagery; a case study from Beds I and II, Olduvai Gorge
856 (Tanzania). *Journal of Archaeological Science* 40 (5), 2446–2457.

- 857 Diggle, P., 1985. A kernel method for smoothing point process data. *Applied Statistics*
858 (Journal of the Royal Statistical Society, Series C) 34, 138–147.
- 859 Domínguez-Rodrigo, M., Bunn, H., Mabulla, A., Baquedano, E., Uribelarrea, D.,
860 Pérez-González, A., Gidna, A., Yravedra, J., Diez-Martin, F., Egeland, C., Barba,
861 R., Arriaza, M., Organista, E., Ansón, M., 2014a. On meat eating and human evolu-
862 tion: A taphonomic analysis of BK4b (Upper Bed II, Olduvai Gorge, Tanzania), and
863 its bearing on hominin megafaunal consumption. *Quaternary International* 322–323,
864 129–152.
- 865 Domínguez-Rodrigo, M., Bunn, H., Pickering, T., Mabulla, A., Musiba, C., Baque-
866 dano, E., Ashley, G., Diez-Martin, F., Santonja, M., Uribelarrea, D., Barba, R.,
867 Yravedra, J., Barboni, D., Arriaza, C., Gidna, A., 2012. Autochthony and orientation
868 patterns in Olduvai Bed I: a re-examination of the status of post-depositional biasing
869 of archaeological assemblages from FLK North (FLKN). *Journal of Archaeological
870 Science* 39 (7), 2116 – 2127.
- 871 Domínguez-Rodrigo, M., Cobo-Sánchez, L., Yravedra, J., Uribelarrea, D., Arriaza, C.,
872 Organista, E., Baquedano, E., 2017. Fluvial spatial taphonomy: a new method for the
873 study of post-depositional processes. *Archaeological and Anthropological Sciences*,
874 1–21.
- 875 Domínguez-Rodrigo, M., Diez-Martín, F., Yravedra, J., Barba, R., Mabulla, A., Baque-
876 dano, E., Uribelarrea, D., Sánchez, P., Eren, M. I., 2014b. Study of the SHK Main
877 Site faunal assemblage, Olduvai Gorge, Tanzania: Implications for Bed II taphon-
878 omy, paleoecology, and hominin utilization of megafauna. *Quaternary International*
879 322–323, 153–166.
- 880 Domínguez-Rodrigo, M., García-Pérez, A., 07 2013. Testing the Accuracy of Different
881 A-Axis Types for Measuring the Orientation of Bones in the Archaeological and
882 Paleontological Record. *PLoS ONE* 8 (7), e68955.
- 883 Domínguez-Rodrigo, M., Uribelarrea, D., Santonja, M., Bunn, H., García-Pérez, A.,
884 Pérez-González, A., Panera, J., Rubio-Jara, S., Mabulla, A., Baquedano, E., Yrave-

- 885 dra, J., Diez-Martín, F., 2014c. Autochthonous anisotropy of archaeological mate-
886 rials by the action of water: experimental and archaeological reassessment of the
887 orientation patterns at the Olduvai sites . Journal of Archaeological Science 41 (0),
888 44 – 68.
- 889 Eren, M. I., Durant, A., Neudorf, C., Haslam, M., Shipton, C., Bora, J., Korisettar,
890 R., Petraglia, M., 2010. Experimental examination of animal trampling effects on
891 artifact movement in dry and water saturated substrates: a test case from South India.
892 Journal of Archaeological Science 37 (12), 3010 – 3021.
- 893 Gabucio, M. J., Fernández-Laso, M. C., Rosell, J., 2017. Turning a rock shelter into a
894 home. neanderthal use of space in abric romaní levels m and o. Historical Biology
895 0 (0), 1–24.
- 896 URL <http://dx.doi.org/10.1080/08912963.2017.1340470>
- 897 García-Moreno, A., Smith, G. M., Kindler, L., Pop, E., Roebroeks, W., Gaudzinski-
898 Windheuser, S., Klinkenberg, V., 2016. Evaluating the incidence of hydrological
899 processes during site formation through orientation analysis. A case study of the
900 middle Palaeolithic Lakeland site of Neumark-Nord 2 (Germany). Journal of Ar-
901 chaeological Science: Reports 6, 82 – 93.
- 902 Gifford-Gonzalez, D., Damrosch, D., Damrosch, D., Pryor, J., Thunen, R., 1985. The
903 Third Dimension in Site Structure: An Experiment in Trampling and Vertical Dis-
904 persal. American Antiquity 50 (4), 803–818.
- 905 Giusti, D., Arzarello, M., 2016. The need for a taphonomic perspective in spatial analy-
906 sis: Formation processes at the Early Pleistocene site of Pirro Nord (P13), Apricena,
907 Italy. Journal of Archaeological Science: Reports 8, 235 – 249.
- 908 Harvati, K., Panagopoulou, E., Tourloukis, V., Thompson, N., Karkanas, P., Athanas-
909 siou, A., Konidaris, G., Tsartsidou, G., Giusti, D., 2016. New Middle Pleistocene
910 elephant butchering site from Greece. In: Paleoanthropology Society Meeting. At-
911 lanta, Georgia, pp. A14–A15.

- 912 Hivernel, F., Hodder, I., 1984. Analysis of artifact distribution at Ngenyem (Kenya):
913 depositional and postdepositional effects. In: Hietala, H., Larson, P. (Eds.), *Intrasite*
914 *Spatial Analysis in Archaeology*. Cambridge University Press, Ch. 7, pp. 97–115.
- 915 Hodder, I., Orton, C., 1976. *Spatial Analysis in Archaeology*. New Studies in Archaeo-
916 *logy*. Cambridge University Press, Cambridge.
- 917 Isaac, G. L., 1967. Towards the interpretation of occupation debris: Some experiments
918 and observations. *Kroeber Anthropological Society Papers* 37 (37), 31–57.
- 919 Jammalamadaka, S., Sengupta, A., Sengupta, A., 2001. *Topics in Circular Statistics*.
920 Series on multivariate analysis. World Scientific.
- 921 Lenoble, A., 2005. Ruissellement et formation des sites préhistoriques. Référentiel ac-
922 tualiste et exemple d’application au fossile. Vol. 1363 of International Series. British
923 *Archaeological Report*, Oxford.
- 924 Lenoble, A., Bertran, P., 2004. Fabric of Palaeolithic levels: methods and implications
925 for site formation processes. *Journal of Archaeological Science* 31 (4), 457 – 469.
- 926 Lenoble, A., Bertran, P., Lacrampe, F., 2008. Solifluction-induced modifications
927 of archaeological levels: simulation based on experimental data from a modern
928 periglacial slope and application to French Palaeolithic sites. *Journal of Archaeo-*
929 *logical Science* 35 (1), 99 – 110.
- 930 López-Ortega, E., Bargalló, A., de Lombera-Hermida, A., Mosquera, M., Ollé, A.,
931 Rodríguez-Álvarez, X. P., 2015. Quartz and quartzite refits at Gran Dolina (Sierra
932 de Atapuerca, Burgos): Connecting lithic artefacts in the Middle Pleistocene unit of
933 TD10.1. *Quaternary International*, –.
- 934 López-Ortega, E., Rodríguez, X. P., Vaquero, M., 2011. Lithic refitting and movement
935 connections: the NW area of level TD10-1 at the Gran Dolina site (Sierra de Ata-
936 puerca, Burgos, Spain). *Journal of Archaeological Science* 38 (11), 3112 – 3121.
- 937 Malinsky-Buller, A., Hovers, E., Marder, O., 2011. Making time: ‘Living floors’,
938 ‘palimpsests’ and site formation processes – A perspective from the open-air Lower

- 939 Paleolithic site of Revadim Quarry, Israel. *Journal of Anthropological Archaeology*
940 30 (2), 89 – 101.
- 941 URL [http://www.sciencedirect.com/science/article/pii/
942 S0278416510000632](http://www.sciencedirect.com/science/article/pii/S0278416510000632)
- 943 Marwick, B., 2017. Computational reproducibility in archaeological research: Ba-
944 sic principles and a case study of their implementation. *Journal of Archaeological
945 Method and Theory* 24 (2), 424–450.
- 946 McPherron, S. J., 2005. Artifact orientations and site formation processes from total
947 station proveniences. *Journal of Archaeological Science* 32 (7), 1003 – 1014.
- 948 Morin, E., Tsanova, T., Sirakov, N., Rendu, W., Mallye, J.-B., Lèveque, F., 2005. Bone
949 refits in stratified deposits: testing the chronological grain at Saint-Cesaire. *Journal
950 of Archaeological Science* 32, 1083–1098.
- 951 Morton, A. G. T., 2004. *Archaeological Site Formation: Understanding Lake Margin
952 Contexts*. No. 1211 in BAR International Series. Archaeopress, Oxford.
- 953 Nickel, B., Riegel, W., Schonherr, T., Velitzelos, E., 1996. Environments of coal forma-
954 tion in the Pleistocene lignite at Megalopolis, Peloponnesus (Greece) - reconstruc-
955 tion from palynological and petrological investigations. *N. Jb. Geol. Palaont. A.* 200,
956 201–220.
- 957 Nielsen, A. E., 1991. Trampling the archaeological record: an experimental study.
958 *American Antiquity* 56 (3), 483–503.
- 959 Ohser, J., 1983. On estimators for the reduced second moment measure of point pro-
960 cesses. *Mathematische Operationsforschung und Statistik, series Statistics* 14, 63–
961 71.
- 962 Organista, E., Domínguez-Rodrigo, M., Yravedra, J., Uribelarrea, D., Arriaza, M. C.,
963 Ortega, M. C., Mabulla, A., Gidna, A., Baquedano, E., 2017. Biotic and abiotic pro-
964 cesses affecting the formation of BK Level 4c (Bed II, Olduvai Gorge) and their bear-
965 ing on hominin behavior at the site. *Palaeogeography, Palaeoclimatology, Palaeo-
966 ecology*, –.

- 967 Orton, C., 1982. Stochastic process and archaeological mechanism in spatial analysis.
968 Journal of Archaeological Science 9 (1), 1 – 23.
- 969 Panagopoulou, E., Tourloukis, V., Thompson, N., Athanassiou, A., Tsartsidou, G.,
970 Konidaris, G., Giusti, D., Karkanas, P., Harvati, K., 2015. Marathousa 1: a new Mid-
971 dle Pleistocene archaeological site from Greece. Antiquity Project Gallery 89 (343).
- 972 Petraglia, M. D., Nash, D. T., 1987. The impact of fluvial processes on experimen-
973 tal sites. In: Nash, D. T., Petraglia, M. D. (Eds.), Natural formation processes and
974 the archaeological record. Vol. 352 of International Series. British Archaeological
975 Reports, Oxford, pp. 108–130.
- 976 Petraglia, M. D., Potts, R., 1994. Water Flow and the Formation of Early Pleistocene
977 Artifact Sites in Olduvai Gorge, Tanzania . Journal of Anthropological Archaeology
978 13 (3), 228 – 254.
- 979 Pierson, T. C., 2005. Distinguishing between debris flows and floods from field evi-
980 dence in small watersheds. Usgs numbered series, U.S. Geological Survey.
- 981 R Core Team, 2016. R: A Language and Environment for Statistical Computing. R
982 Foundation for Statistical Computing, Vienna, Austria.
- 983 Rick, J. W., 1976. Downslope movement and archaeological intrasite spatial analysis.
984 American Antiquity 41 (2), 133–144.
- 985 Ripley, B., 1977. Modelling spatial patterns. Journal of the Royal Statistical Society,
986 series B 39, 172–212.
- 987 Ripley, B., 1988. Statistical inference for spatial processes. Cambridge University
988 Press.
- 989 Ripley, B. D., 1976. The second-order analysis of stationary point processes. Journal
990 of Applied Probability 13 (2), 255–266.
- 991 Ripley, B. D., 1981. Spatial Statistics. John Wiley and Sons, New York.

- 992 Schick, K. D., 1984. Processes of paleolithic site formation: an experimental study.
993 Ph.D. thesis, University of California, Berkeley.
- 994 Schick, K. D., 1986. Stone Age sites in the making: experiments in the formation
995 and transformation of archaeological occurrences. Vol. 319 of International Series.
996 British Archaeological Reports, Oxford.
- 997 Schick, K. D., 1987. Modeling the formation of Early Stone Age artifact concentra-
998 tions. *Journal of Human Evolution* 16, 789–807.
- 999 Schiffer, M. B., 1972. Archaeological Context and Systemic Context. *American Antiq-*
1000 *uity* 37 (2), 156–165.
- 1001 Schiffer, M. B., 1983. Toward the identification of formation processes. *American An-*
1002 *tiquity* 48 (4), 675–706.
- 1003 Schiffer, M. B., 1987. Formation processes of the archaeological record. University of
1004 New Mexico Press, Albuquerque.
- 1005 Shackley, M. L., 1978. The behaviour of artefacts as sedimentary particles in a fluvialite
1006 environment. *Archaeometry* 20 (1), 55–61.
- 1007 Sisk, M. L., Shea, J. J., 2008. Intrasite spatial variation of the Omo Kibish Middle Stone
1008 Age assemblages: Artifact refitting and distribution patterns . *Journal of Human*
1009 *Evolution* 55 (3), 486 – 500.
- 1010 Sánchez-Romero, L., Benito-Calvo, A., Pérez-González, A., Santonja, M., 12 2016.
1011 Assessment of Accumulation Processes at the Middle Pleistocene Site of Ambrona
1012 (Soria, Spain). Density and Orientation Patterns in Spatial Datasets Derived from
1013 Excavations Conducted from the 1960s to the Present. *PLOS ONE* 11 (12), 1–27.
- 1014 Todd, L., Stanford, D., 1992. Application of conjoined bone data to site structural
1015 studies. In: Hofman, J., Enloe, J. (Eds.), *Piecing Together the Past: Applications of*
1016 *Refitting Studies in Archaeology*. Vol. 578 of International Series. BAR, Oxford, pp.
1017 21–35.

- 1018 van Vugt, N., de Brujin, H., van Kolfschoten, M., Langereis, C. G., 2000. Magneto-
1019 and cyclostratigraphy and mammal-fauna's of the Pleistocene lacustrine Megalopo-
1020 lis Basin, Peloponnesos, Greece. *Geologica Ultrajectina* 189, 69–92.
- 1021 Vaquero, M., Bargalló, A., Chacón, M. G., Romagnoli, F., Sañudo, P., 2015. Lithic re-
1022 cycling in a Middle Paleolithic expedient context: Evidence from the Abric Romaní
1023 (Capellades, Spain). *Quaternary International* 361, 212 – 228.
- 1024 Vaquero, M., Chacón, M. G., García-Antón, M. D., de Soler, B. G., Martínez, K.,
1025 Cuartero, F., 2012. Time and space in the formation of lithic assemblages: The
1026 example of Abric Romaní Level J. *Quaternary International* 247 (0), 162 – 181.
- 1027 Villa, P., 1982. Conjoinable Pieces and Site Formation Processes. *American Antiquity*
1028 47 (2), 276–290.
- 1029 Villa, P., 1990. Torralba and Aridos: elephant exploitation in Middle Pleistocene Spain.
1030 *Journal of Human Evolution* 19 (3), 299 – 309.
- 1031 Villa, P., Courtin, J., 1983. The interpretation of stratified sites: A view from under-
1032 ground. *Journal of Archaeological Science* 10 (3), 267–281.
- 1033 Voorhies, M., 1966. Taphonomy and population dynamics of an early Pliocene verte-
1034 brate fauna, Knox County, Nebraska. Ph.D. thesis, University of Wyoming.
- 1035 Walter, M. J., Trauth, M. H., 2013. A {MATLAB} based orientation analysis of
1036 acheulean handaxe accumulations in olorgesailie and kariandusi, kenya rift. *Jour-*
1037 *nal of Human Evolution* 64 (6), 569 – 581.
- 1038 Wood, R. W., Johnson, D. L., 1978. A survey of disturbance processes in archaeologi-
1039 cal site formation. In: Schiffer, M. B. (Ed.), *Advances in archaeological method and*
1040 *theory*. Vol. 1. Academic Press, Ch. 9, pp. 315–381.
- 1041 Woodcock, N., Naylor, M., 1983. Randomness testing in three-dimensional orientation
1042 data. *Journal of Structural Geology* 5 (5), 539 – 548.